雪粒子による視程変動の研究*
(和文概要)

石　本　敬　志**
(平成７年２月受理)

１章：概要

人の眼が，目標物を背景から識別できる最大距離を，気象学的な視程と定義しているが，この場合は，静的現象を想定している。大気の静的現象の表現としてはこれでも問題がないが，降雪時や吹雪の時，目標物を識別する困難さを想像してもわかるように，視程は空間的にも一様ではなく，更に時間的変動をも含む場合が多い。自分の眼で状況を確認できる視覚は，車の運転者にとって最も重要な情報源である。この，視覚情報の円滑な取得を妨げているのが視程障害であり，空間的な否一様性と，空閤浮造物による時間変動の研究を行った。

２：視程計測原理と野外観測

目標物を背景から識別できる最大距離が視程の定義であるが(Koschmieder)，透過率でも光の減衰を計測できるので（竹内)，透過率計を用いて視程の連続測定が可能である。輝度差でも，透過率でも分解能が最も良くなる光の投受光間隔は，計測する視程距離の１／３であることが解析的に導ける。

３章：空間浮遊粒子よる視程減衰

霧は，吹雪などに比べ一様に分布していることを反映し，平均視程は低下するものの，変動強度は小さい。透過率計で測定された降雪の視程変動スペクトルは，周期の短い部分でピークを持つが，その変動レベルは吹雪の１／１０００程度である。吹雪では，周期が短く大きな変動幅で視程が変動する。このため，路面が雲水路面の時，平均視程が同じでも車の速度に与える影響が異なり，吹雪時の視程と車の速度は負の相関を持っている。

４章：車による雪煙の発生機構とその大きさ

温度が下がるほど雪粒子の結合力が弱くなるため，車の周囲にできる伴流や，タイヤの機械的な力で雪が舞い上がる。こうした，雪煙の発生しやすさは，気温と降雪量から大まかに推定できる。また，雪煙の高さは雪粒子の落下速度と車の周りにできる伴流の垂直速度成分の大きさと均衡していると説明でき，一台の車による雪煙の高さは，ほぼ車の高さと同じ程度になることが説明できる。

５章：霧・降雪と吹雪・車による雪煙の識別

霧・降雪・吹雪・雪煙などによる視程距離の減衰・変動の特徴を調べ，視程計による測定から変動強度を計算し，霧・降雪と吹雪・雪煙を識別した。視程変動強度の計算は，視程を対数表現した方が，実態に合った説明が可能である。

---

*本稿は北海道大学審査学位論文である。
**防災雪氷研究室長

６章：輝度差を用いた視程計測システムの開発

Koschmieder の定義通り，背景と目標物の輝度差から視程を計測した。また，この原理を用いて，CCD ビデオカメラをセンサーとする視程計測システムを開発した。この計測システムは一点から複数箇所の視程を０．５秒毎に同時計測できる唯一のシステムである。このシステムによって，人の眼のように一点から複数箇所を見たときの視認距離を同時測定できるようになった。

７章：視程障害対策による視程障害緩和機構

防雪柵は風下の風速を弱め，強い風によって運ばれる雪の量を減らし，視程の急な減衰を緩和する。３列の防雪林の風下で行った飛雪流量や視程の観測から，風が強く吹雪による飛雪量が増えるほど，防雪林設置効果が大きくなる。

8 章：結論

霧・降雪・吹雪・雪煙などによる視程障害の特徴を明らかにするとともに，輝度差による視程計測原理をＣＣＤビデオカメラに適用し，一点から多測点の視程を同時測定可能なシステムを関発した。今後は視程障害を引き起こす要因と現象の相互関係や気象学的な背景を調べ，関連分野研究者との協力を深め視程障害の予知を可能にしたい。

STUDIES ON THE VISIBILITY FLUCTUATION AIRBORNE SNOW PARTICLES

by
Keishi Ishimoto

CONTENTS

1. INTRODUCTION

The number of traffic accidents involving many vehicles has been increasing in attenuated visibility condition in winter. The largest number of traffic accidents in Japan occurred in snowy season in Hokkaido in 1992. Sudden attenuation of visual range by falling snow was reported at that time. Dynamic visual acuity reduces with age and higher speed of vehicles. Study on visibility fluctuation is becoming more important to keep safe transportation.

Although visibility is defined for static conditions in meteorology, characteristics of visibility attenuation depend on mass flux of airborne particles. Visibility fluctuates a little in falling snow and fog, but varies greatly both spatially and temporally in blowing snow and vehicle-generated snow clouds. Although it is difficult to observe and record visibility continuously by human eye, A visibility meter can be used to monitor visual range directly･

The following topics are investigated in this paper.

1)The characteristics of visibility attenuation in fog, falling snow and blowing snow.

2)The mechanism, size and triggering condition of vehicle-generated snow cloud.

3)The discrimination among fog, falling snow, blowing snow and vehicle-generated snow clouds.

4)A new visibility measuring system using brightness contrast that can measure visibility of six arbitrary points from one viewpoint in the scene of a CCD camera every 0.5 second.

2. THE PRINCIPLE OF VISIBILITY OBSERVATION AND F正LD OBSERVATION

2.1 INTRODUCTION

Visibility is defined as the greatest distance in a given direction at which it is just possible to see and identify with unaided eye (a) in the daytime, a prominent dark object against the sky at the horizon, and (b) at night, a knownn, preferably unfocused, moderately intense light source(l). Visual range, on the other hand, signifies the distance that something can be seen(2). A comparison of calculated visibility with visual range as sensed by the human eye shows that the transmissometer can be used to measure visibility in blowing snow(3). According to Takeuchi(3), visibility relates more with mass flux than with volumetric density of airborne snow particles.

2.2 EXPRESSION OF VISUAL RANGE

Visibility meters may be classified into two broad types. One includes devices which can monitor the brightness contrast between an object and the surroundings. The other includes devices which monitor a limited volume of air as a transmissometer. The latter is more popular than the former because it is easy to operate for continuous monitoring and has a clear theoretical background(3). Visual range is derived as follows. If the luminance of the target is Bd and that of the background is Bh, the contrast C is defined as:

$$C=(B_d-B_h)/B_h \qquad (1)$$

where Bd is the luminance of the object d (m) separated from the luminance meter, and Bh is the horizontal background luminance. Duntley (1948) expresses the contrast attenuation as:

$$\frac{C}{C_0}=e^{-\sigma d} \qquad (2)$$

where o is the light attenuation coefficient. C_0 is the contrast at the luminance meter. Koschmieder(1924) defines the visual range (V)as the distance at which the brightness contrast reaches the threshold (e is the threshold of the brightnes-contrast, e = 0.05, in highway meteorology):

$$e=e^{-\sigma v} \qquad (3)$$

Consequently, the visual range V(m)was derived from the brightness contrast as:

$$V=d\ \ln(e)/\ln(c/c_0) \qquad (4)$$

where d is the distance from the luminance meter to the target.

Bouguer's law expresses the light attenuation coefficient as:

$$\sigma = d^{-1} \ln(1/T) \qquad (5)$$

where T is the transmissivity. The visual range through the transmissometer is:

$$V = d \ln(e)/\ln(T) \qquad (6)$$

The desirable distance from the sensor to the target is calculated to get the most accurate visual range The relative error is:

$$\frac{\Delta V}{V} = \frac{T^{-1}}{\ln T^{-1}} \Delta T = \frac{e^{3dV^{-1}}}{3dV^{-1}} \Delta T \qquad (7)$$

If △T is the preset accuracy of the transmissivity, one can show that △V/V has a minimum at 3 d/V = 1; Hence, the most accurate measure of visual range occurs when the base line is of the order of 1/3 of the expected visual range, we can get the most accurate visual range(4). Most adequate span of a transmissometer varies according to visibility to observe as shown in Figure 1(3).

When using a transmissometer, enough space without optical obstacles must be provided, and it must be set firmly to provide a stable optical axis. Therefore, a reflector-type visibility meter is more popular on highways. The output voltage (V_0) from a reflector-type visibility meter was compared with the visibility measured with a transmissometer-type visibility sensor(Figure 2)(5). Visual range (V)is calculated by:

$$V = 26.33 V_0^{-0.87} \qquad (8)$$

2.3. OBSERVATION STATIONS

Figure 3 shows the locations of observatory stations of the Civil Engineering Research Institute of Hokkaido Development Bureau. Road weather involving visual range was observed at Ebetu, National Highway Route(NHR)12 and Douou expressway. Another permanent road weather observation station is located at Nakayama mountain pass on NHR 230.

At Ishikari station, basic studies were carried out as following :

1) Comparison between visual range through a luminance meter and a transmissometer-type visibility meter.
2) Relation between a reflector-type visibility meter and a transmissometer-type visibility meter.
3) Development of CCD camera-type visibility meter.
4) Airborne snow particle size in blowing snow.
5) Surface condition of snow cover in blowing snow using a thin section analysis.

Visibility fluctuations in fog, falling snow and blowing snow were observed at Nakayama mountain pass of 800 m in elevation.

The trigger condition and the mechanism of vehicle-generated snow cloud were observed at Ebetu. The improvement of reduced visual range was observed at Ebetu and Iwamizawa on NHR 12,

2.4 DATA ACQUISITION AND TRANSMISSION SYSTEM

Data observed in field is recorded every 0.1 - 0.2 second using personal computers with A/D converter and hard disk or magnetic tape recorder for the higher frequency recording. Every 10 minutes data average is transmitted to our institute via NTT telephone network to monitor our observation system and to help make decisions regarding additional observations.

3. VISIBILITY ATTENUATION BY AIRBORNE PRECIPITATION PARTICLES

3.1 INTRODUCTION

Characteristics of visibility attenuation are influenced by the physical properties and spatial and temporal distributions of airborne precipitation particles. As a result, visual range of drivers is affected by visibility fluctuations. In this study, the visibility fluctuation in fog, blowing snow and vehicle･generated snow cloud were analyzed and compared with each other.

3.2 VISIBILITY IN FOG

Fog occurs when clouds extend to the ground i mountainous areas like the Nakayama mountain pass NHR 230. Airborne particles in fog are smaller than airborne snow particles and are adequately diffused and distributed homogeneously in the atmosphere. Figure 4 shows visual range and wind speed in time series. Wind speed in fog is typically lower than that in blowing snow, and the fluctuation of visibility in fog is therefore less than that in blowing snow. Visual range is reduced but stable in such foggy condition. The mass flux of blowing snow increases in logarithmic scale when approaching ground level(6). The distribution of snow particles depends on wind speed and topography. The peak of the power spectrum as shown in Figure 5 is lower than 0.1 Hz.

3.3 VISIBILITY IN BLOWING SNOW AND FALLING SNOW

Visual range fluctuates according to falling snow intensity, wind speed and topography in blowing snow. Figure 6 shows a time series of visual range and wind speed in blowing snow on Nakayama mountain pass along NHR 230. Visual range in blowing snow fluctuates more than that in fog as described previously. The power spectrum of visibility in blowing snow (Figure 7) has a peak of nearly 1 0 Hz, and is therefore 1 00 times larger than that in fog

Visual range and wind speed in falling snow are shown in Figure 8. Mean visual range is almost stable with little fluctuation. Although the power spectrum of visual range has a peak in high frequency, the power is not as large as that in blowing snow (Figure 9).

Wind carries snow particles which reduce visibility.

Cross-correlation (Rxy) between wind speed and visibility at 0.2m above snow surface was calculated as shown in Figure 10.

$$R_{xy}(\tau) = \overline{X(t)\,Y(t+\tau)} / \sqrt{\overline{X^2}}\sqrt{\overline{Y^2}} \qquad (9)$$

where $X(t) = w(t) - \bar{w}$

$Y(t) = V(t) - \bar{V}$

where t is time; τ is time lag; X(t) is wind fluctuation, and Y(t)is visual range fluctuation every 0.5 second for 20 minutes at 0 2 m above snow surface. Sudden violent rush of wind was followed by reduced visibility a few seconds later. Mean wind speed was 6 m/s and mean visibility was 165 m, Downward arrow denotes zero-lag time by considering the distance between the light-pass and the anemometer.

Tabler mentioned characteristics of visual range attenuation in blowing snow in relation to motorist vision(7). He derived the equation to estimate visual range as a function of wind speed and pointed out the relationship between gust frequencies in space and time.

4. MECHANISM AND SIZE OF VEHICLE-GENERATED SNOW CLOUD

4.1 INTRODUCTION

The cohesion of snow particles on a road surface is destroyed by the mechanical action of vehicle tires and the shear stress exerted in the wake by moving vehicles. Therefore, the visibility will be decreased and the number of traffic accidents will be increased by the vehicle-generated snow cloud without appropriate countermeasures against reduced visibility･

4.2 THRESHOLD OF REDUCED VISUAL RANGE CAUSED BY SNOW ENTRAINMENT IN VEHICLE WAKES

Figure 11 shows the threshold condition of blowing snow with precipitation(S). Bonding of snow particles tends to increase with temperature. Figure 12 shows the reduction of visibility by vehicle-generated snow clouds in relation to temperature and precipitation. Precipitation increases visibility attenuation in the wake of moving vehicles. As the temperature drops, the cohesion of snow particles decreases, causing them to be blown up from the road surface more readily. While the threshold wind speed of heavy blowing snow has less relation to temperature, reduced visibility in vehicle-generated snow cloud varies greatly with temperature.

A snow cloud generated by a large truck in the passing lane is shown in Figure 1 3, 1n this case, the wind was calm soon after precipitation ended, the sky was clear, and the air temperature was -4 °C. Although the road had been plowed and the travel lane was mostly bare, a little snow still remained on the passing lane.

The monthly mean air temperature in Hokkaido from December l to April l typically ranges between -10 and 0°C. The threshold of vehicle-generated snow clouds depends on air temperature. Besides real-time meteorological data, forecasts for precipitation and air temperature are also available from on-line meteorological services. If one knows the correlation between the threshold for snow entrainment in vehicle wakes and the air temperature and precipitation, it is possible to provide the motoring public with information on adverse conditions caused by vehicle-generated snow clouds.

4.3 SIZE OF AIRBORNE SNOW PARTICLES

Granular snow particles on highways soon after snowfall are smaller than those of falling snow (9). According to previous studies concerning snow on highways, the sizes of snow particles range from 50 to 300 μm in diameter and the shape is round when compared with new fallen snow crystals, The size of melted snow particles in blowing snow was observed on the glass slide covered with oil as shown in Figure 14, Figure 15 (a) shows the size distribution of snow particles size obtained by this method, and Figure 15 (b) shows the distribution as observed by a snow particle counter (10). Statistical tests indicate that both distributions are samples from the same population. For practical applications snow particle counters can be used for real time observation of airborne snow particles on highways. Figure 1 6 shows the size distribution of snow particles on a highway in blowing snow (*left* and *middle*) and in vehicle-generated snow cloud(*right*)(U). These data were obtained on Douou expressway Sapporo and Iwamizawa. In the vehicle-generated snow clouds, the number of smallei snow particles was greater than that in blowing snow. No particle larger than 250 μm in diameter was found.

4.4 SURFACE FABRIC OF SNOW COVER AND DEVELOPMENT OF BLOWING SNOW

The surface fabric of the snow cover varies with the development of blowing snow. We car observe the development process of blowing snow before freezing of the river surface at Ishikari river site. The river width is over 300 m as shown in Figure 17, Most of the snow particles from the

windward side drop into the river before reaching the leeward side. Then we can observe the developing process of blowing snow and changes of the surface fabric of snow cover on the flooding area of the Ishikari river. Snow samples for thin sections were used to observe the surface fabric snow cover after several hours of blowing snow with precipitation. Figure 18(A)shows the thin section(A) of snow cover at a point 10 m from the edge ofopen water of the river, and Figure 18(B) shows the thin sections(B) of snow cover 300 m from that point. More porosity was observed in the thin section near the edge of open water of the river than at the downwind location when the porosity between snow fabrics is filled with smaller snow particles carried. Speed of sintering is higher in smaller snow particles. Wind pack effect is predominant and the strength of snow particle bonding increases with increasing distance of snow transport. Tabler pointed out that older snow consists of grains sintered to form a surface relatively resistant to particle dislodgment. Fresh snow, however, is quickly fragmented and easily transported(7).

4,5 DURATION AND SIZE OF VEHICLE-GENERATED SNOW CLOUD RELATED TO HIGHWAY DESIGN

The diffusion of a vehicle-generated snow cloud is influenced by the geometry of the road and nearby structures. The duration of snow in the wake of vehicles is defined as the period fi ° om the time when visual range is reduced below 300 m to the time when the visual range recovers to 300 m, Visual range caused by snow in the wake of a large truck lasted longer than 60 sec on NHR 1 2 at a location along a river embankment with 5-m-high snow fence 10 m upwind(Figure 19). At this location, the embankment and snow fence delayed the diffusion of snow in the wake. In comparison, the visibility measured by a reflector-type sensor on the median ofNHR 40 showed the duration of reduced visual range to be only about 10 sec as shown in Figure 20. At this location, snow particles in vehicle-generated snow clouds are dispersed more quickly. Figure 21 shows the cross sections ofNHRs 12 and 40(12). During both observations the air temperature was -9°C and the wind velocity was about 1 m/s.

Visual range reduced by snow in the wake of small vehicles was observed on NHR 40 at the same time as shown in Figure 22 (air temperature of -9.6°C and mean wind speed of 1.1m/s). The duration of snow clouds was about 5 sec at the observation point. Minimum visual range was 40 % greater than that associated with the snow cloud generated by a large vehicle. Larger wakes formed by large vehicles cause poorer visual range lasting longer period than those formed by small vehicles.

The wake generated by vehicles has been investigated in relation to air pollution. The height of wake l was estimated as following:

$$l \propto \gamma A h (X/h)^{1/4} \qquad (10)$$

where X is the distance behind the vehicle. A is the cross section area of the vehicle, and γ is a constant of the same order as Karmaris constant. The height of the wake expressed by Equation (10) agrees with the observed results in the field (13). The height of a vehicle-generated wake given by Equation (10) reaches several times the height of a vehicle as shown in Figure 23, however, that of a vehicle generated snow cloud as shown in Figure 24 does not. The photograph (Figure 24)taken on the Douou express way illustrates this phenomenon.

Snow particles in a vehicle-generated snow cloud were smaller than 250 μm, and that value is smaller than falling snow crystals reported by Kinoshita (8). Terminal falling velocity is on the order of several tens of cm/s. Eskridge (13) reported that the height of vertical wind fluctuation reaches several tens of cm/s at the height of a vehicle roof (Figure 23). Therefore, Vertical wind fluctuation supports falling snow particles in snow clouds generated by vehicles.

5. DISCRIMINATION BETWEEN FOG, FALLING SNOW, BLOWING SNOW AND VEHICLE-GENERATED SNOW CLOUD

5.1 INTRODUCTION

Dynamic visual range has typical fluctuation in fog, falling snow, blowing snow and vehicle-generated snow clouds. Dynamic range and n ‘ equency of visual range fluctuations vary more in the case of blowing snow than in fog. Vehicle speed was averaged for 1 0 minutes duration in several hours and compared with visual range by a reflector-type visual range meter on Nakayama mountain pass on NHR 230 as shown in Figure 25. Road surface was covered with compacted snow both in fog and blowing snow. The correlation coefficient between visual range (visibility) and vehicle speed was 0.25 in fbg。and 0.65 in blowing snow. We confirmed this tendency in 1992(Figure 26) during the periods January to March, November to December when the road surface was covered with compacted snow or ice, wind speed averaged for 10 min. was over 8 m/s. The correlation coefficient between vehicle speed and visibility was 0.65.

A significant correlation exists when wind averaged for 10 min. is over 8 m/s and road surface

is covered with compacted snow or ice. Figure 27 shows the relation between vehicle speed and visibility involving all data in the same period for conditions of compacted snow or icy road surface. There is no correlation between visibility and wind speed. We can get more information from visual range data if we can discriminate fog, falling snow, blowing snow. and vehicle-generated snow cloud. Tabler(7) mentioned that the large visual range fluctuation affects transportation.

5.2 NEW EXPRESSION OF DISCRIMINATION BETWEEN PRECIPITATION PARTICLES

According to Weber-Fechner's law(14), any human sensitivity including that to visual range, is scaled logarithmically. The intensities of visual range fluctuation on linear and logarithmic scales are given by equations (11) and (12), respectively. The fluctuation intensities calculated by those two methods are compared under various conditions by using data sampled every 0.01 second for every 20 minutes(Table 1).

$$I(\%) = \frac{\sqrt{\overline{(V-\bar{V})^2}}}{\bar{V}} \cdot 100 \qquad (11)$$

$$IL(\%) = \frac{\sqrt{\overline{(\log(V)-\overline{\log(V)})^2}}}{\overline{\log(V)}} \cdot 100 \qquad (12)$$

From the calculated results ofboth equations (10) and (11), visibility fluctuated more in blowing snow and in vehicle-generated snow clouds, than it did in calm, falling snow and foggy conditions. The linear-scale fluctuation intensities tend to decrease as visibility reduces n ‘ om 305 to 40 m, but the logarithmic values remain constant over this range. This suggests that the logarithmic scale may coincide better with human sensitivity, and therefore provides a better index for visual range reduction. The intensity of fluctuations calculated by either method can be used to distinguish blowing snow, vehicle-generated snow cloud from fog, and falling snow in calm condition.

6. VISIBILITY MEASURING SYSTEM USING BRIGHTNESS CONTRAST

6.1 INTRODUCTION

Visual range is defined as the greatest distance at which an object can be seen and identified. In accordance with Koschmieder's theory, the apparent brightness of a black object, with baffles covered by black cloth, was compared simultaneously with the apparent brightness of background sky near the target in Ishikari (Figures 28,29 and 3 0), and the visual range was derived by equation(4). The visual range observed by a pair of luminance meters was compared with that by a transmissometer (4). The luminance of background (snow cloud in sky) varied from 5o00 cd (candela) to 20000 cd.

Visibility through the transmissometer and luminance meter was recorded at an interval of 0. 1 seconds and compared with each other (Figure 31). The visual range through the transmissometer was usually greater than that through the luminance meter. Wave length of the luminance meter is similar to that of human sensitivity. Both transmissometer-type and reflector-type visibility meters use modulated ultra red light. However, visual range observation using luminance meter is considered more ideal. hence a new visual-range monitor has been developed based on this principle. However the luminance meter method has a problem of keeping the absolutely black area of the target from being affected by the surrounding brightness to ensure accurate evaluation. The new system we have developed compensates for the effects ofthe brightness of the su冫丁oundings by keeping the absolutely black area within the lens of the video camera.

A new visibility-range measuring system has been developed which uses a video camera with an optical filter similar to the human eye. Using this system, visual range can be estimated by measuring the brightness contrast of a black target against a standardized background as described below(15).

6.2 INSTRUMENTATION AND FIELD OBSERVATION

The development of CCD video cameras has made it possible to overcome most of the long-standing operational shortcomings of tube type video cameras(16) such as distortion of the image due to its position in the visual field and high-light intensity burn-in and after images. The CCD image sensor used in our study was composed of an array of 384 × 491 cells charged in proportion to the intensity of the illumination of their cells. Thus, the CCD video camera was able to measure the brightness of any chosen area visible within its range.

A half-black and half-white plate was used as a target with the CCD video camera. The white area of the target represented the surrounding brightness and was so illuminated as to make possible the measurement of visibility at night. The three targets were set up 30 m apart and at heights of a 0.45, 1,1.5 m above the snow surface to observe visual range simultaneously at three different levels.

These targets were placed in parallel with the prevailing wind direction, and were painted with an anti-reflecting paint to avoid reflection from the snow surface. The lay-out diagram of the monitoring system is shown in Figure 32. Observations corresponding to a visibility range of 0-990 m could be made using an output voltage of 1 - 5 V, Parameters were changed as required by adjusting the monitor. The lens with auto-iris can respond to brightness over the full visual range and is therefore capable of monitoring all possible conditions. The behavior of the auto-iris itself can be monitored by the CCD control unit that reduces the effects of the surrounding brightness on the brightness of the target.

During 1987 and 1988, this monitoring system and a transmissometer were set up at a height of 1.5 m above the snow surface at the blowing snow observation station of the Civil Engineering Research Institute ofHokkaido Development Bureau in Ishikari. The light pass of the transmissometer was 15 m ahead of that of the CCD video camera along the prevailing wind direction. The air temperature, wind speed and wind direction were recorded simultaneously in the field. The field instrumentation of the video camera and the three targets are shown in Figure 3 3 ・

In addition to the use of these devices, visibility to the human eye was assessed by using seven black targets of a size equal to half the visual angle from the observation point to the recording apparatus shown in Figure 28. The luminance of the black and white areas of the target in the scene of the monitor are used to calculate visual range, and are introduced into the system after adjusting the luminance of surroundings. A series of adjusting process was needed to get accurate visual range in twilight conditions.

The relationship between visibility and transmissivity is derived from Koschmieder's equation and Bouger-Lambart law as Equation (6). The visual range detected through the CCD camera is expressed as Equation (4).ln any experiment using this system, the brightness of the targets depends on a number of other factors in addition to the presence of airborne snow particles, and these additional parameters were used to correct the visibility-range values obtained through the CCD camera. In some cases, automatic correction was made by the automatic iris, and in others adjustments were made through the keyboard of the parameter-setting monitor. Maximum possible brightness of the white area of the target was allowed for in this way. The revised algorithm of Equation (4)for considering surrounding brightness is:

$$C=(B_d-B_h)/B_h, \quad C_0=(B_0-B_h)/B_h \qquad (13)$$

where Bh is the brightness of the background; Bo is the brightness of the target at the CCD video camera, and Bd is the brightness of the target at d(m)from the CCD video camera. A further experimental equation can be obtained for the black area of the target:

$$B_0 = (B_{max} - (B_{do} - B_{min})\,C) \qquad (14)$$

where Bmax and Bmin are the maximum and minimum values of brightness for the black area of the target. Bdo is the brightness of the black area of the target at the luminance meter. Bdo is monitored within the lens of the video camera, and C is the constant to exclude the effect of surrounding brightness for values of Bmax = Bmin = 0, and C = -1. Additional algorithms for use in twilight and at night are being developing. These algorithms must be able to adjust automatically in response to changes in the brightness of the surroundings. One of the daytime analyses that we have made is shown in the next section of this paper. The analysis was made as a means to illustrate the comparison between the visibility data obtained from the CCD video camera and by the use of a transmissometer.

6.3 CERTIFICATION OF THE NEW SYSTEM AND A BASIC OBSERVATION

The time interval between the readings in the collection of our data was 0.2 s. A typical example of our observation in blowing snow is shown below. The trend in visibility change with time as observed through the CCD camera was compared with that identified by the transmissometer(Figure 34). Figure 35 shows the visibility by a transmissometer versus that by the CCD camera. The lens of the CCD camera by means of optical filter eliminates the wave of light that the human eye cannot sense. Visibility by a transmissometer is larger by a factor of two than that by a CCD camera. Because the transmissometer was located 15 m ahead of the video camera in the windward direction, the time lag of the visibility fluctuation due to difference of observatory locations had to be corrected to allow for a precise comparison of the readings obtained. The cross-correlation coefficient between visibility at the CCD camera and visibility at the transmissometer, Rxy(γ)is defined by the equation

$$R_{xy}(\tau) = \overline{X(t)\,Y(t+\tau)} / \sqrt{\overline{X^2}}\sqrt{\overline{Y^2}} \qquad (14)$$

where $X(t) = V(t) - \bar{V}$

$Y(t) = V(t) - \bar{V}$

where t is time; τ is time lag; X(t) is the visibility fluctuation by the transmissometer, Y(t)is the visibility fluctuation recorded by the CCD camera, and V(t), v are the instantaneous and the mean ranges of visibility, respectively.

Figure 36 shows the results derived from Equation 13, and from these it can be seen that Rxy(τ) has the maximum value of 0.7 at τ = 1,5s; the mean wind speed at l m above the snow surface measured by an ultrasonic anemometer was 10 m/s ; air temperature at l m height was - 4 ℃; the time lag, τ=1.5 s, corresponds to the difference in length of the path of light to the transmissometer and that to the video camera; mean wind speed was 10 m/s,

Visual range at any location depends on the presence or absence of airborne particles at any particular levels above the snow surface in blowing snow. In our experiments, targets were located at three different levels: A = 2 m, B = 1m, C = 0.45 cm. Visual range fluctuation slower than 1 Hz is considered to be insignificant irritation to human eye (16). The intensity of fluctuation in visual range was calculated using Equation (10) after the process through a numerical filter that admits only frequencies above 0.1 Hz. In Equation(10), V is the instantaneous visual range taken as running mean ofthe visual range for 10 sec.

The magnitudes of fluctuations in visual ranges obtained from our observations were 24 %at 2 m ; 29 % at 1 m ; and 37 % at 0.45 m. Appearance frequency is defined as the ratio of the sum of the time intervals for each degree of visual range during each observation; the division of visual range is 50 m, and the appearance frequencies at the three levels of observation are shown in Figure 37. From this figure it can be seen that the frequencies of the poorer visual ranges at the lowest observation had higher values than those at upper observation levels.

6.4 VERTICAL PROFILES OF VISIBILITY FROM ONE VIEW POINT

No other equipment is capable of observing visibilities of several points from one view point like the human eye. The CCD video camera was set at 55.5 km post on Douou expressway to observe visual range profile at the roadside of the windward lane. Three pairs of black and white boards were set at 0.5, 1.5 and 2.0 m above the snow. The height of the embankment at the observation point is

over 10 m. Wind tended to join together on the top of the embankment slope with airborne snow particles. The visual range of the lowest height began to decrease in the early stage of blowing snow and reached the lowest level of the three heights(Figure 38). Visual range fluctuated according to the height of the target on the roadside.

6.5 CONCLUSIONS REGARDING TO VISIBILITY MEASURING SYSTEM USING CCD VIDEO CAMERA

The visibility-range monitoring system using a CCD video camera that we have developed can measure the visibilities at up to six positions within the range of the video camera, and give information about visual range simultaneously with its observation. The physical features in the vicinity of major roadways are usually complicated compared with those of snow plains. Thus, the range of visual range in regions with major roadways is influenced by the nature of the surroundings and their height above snow surface. Using the system described here, we have been able to monitor simultaneously, at one second intervals, visual ranges at six different points.

For readings taken in the daytime, visibilities measured by the CCD camera coincide with those recorded through a transmissometer-type visual range monitor. The system reported here allows the video camera to monitor the visual range.

7. MECHANISM OF THE IMPROVEMENT OF REDUCED VISUAL RANGE
7,1 INTRODUCTION

One counter measure against reduced visual range is to reduce the mass flux of blowing snow using a snow fence, snow break forest, or a modified highway cut. Other measures include providing a better visual guide along the highways, spreading a chemical to increase adhesion between snow particles on highways.

7.2 SNOW FENCE AND SNOW BREAK FOREST

The number of snow break forests is increasing after our experiments on NHR 12 in Iwamizawa(18).Even a narrow vegetation with 3 or 4 rows of pine decreases wind speed and mass flux. For example, pine trees 3.6 m tall planted along the highway reduced wind speed behind the vegetated section to 10 % of the upwind value. Conversely, wind speed is accelerated on snow

embankment in no-vegetated section along a highway as shown in Figure 3 9.

Mass flux was reduced at the vegetated section as shown in Tables 2 and 3. Mass flux in the forest section was reduced to 10 - 20 % of that in a non-vegetated section. Transmissometer-type visibility meters were set on the medians in both sections on NHR 12. Visibility was analyzed as shown in Table 4. Ten-minutes averaged visibility and intensity of visibility are compared in both sections. The rate of improvement is defined as the value in the vegetated section divided by that in the no-vegetated section. The rate of improvement increases in proportion to the decreasing averaged visibility and the intensity of visibility (17).

Vegetation along highways not only reduces mass flux of blowing snow but also provides better visual guide than conventional roadway delineators during the daytime. Figure 40 shows the snow break forest at Iwamizawa along NHR 12. Figure 41 shows an observation of blowing snow with precipitation in Ebetu, on NHR 12, where visibility on the median on a road and wind speed at 10 m height changed rapidly. On a section without snow fence, visibility was reduced to several tens of meters three times for 2.5 minutes soon after gust. On a section with a 5-m-tall snow fence without bottom gap, visibility did not vary as much and remained greater than 100 m. Mean visibility was 107 m and 127 m respectively. Visibility was the same in both sections when wind speed was below 5 m/s.

7.3 THE EFFECT OF VISUAL CLUES

Roadside vegetation shields highways from wind, ddiffuses snow flux, and improves visual range. Narrow tree plantings can sometime work as a sign clue. Visual range to illuminated delineators was compared with that to pine trees located at the same distance 40 to 80 m away from the observation point in blowing snow. A reflector-type visibility meter was set at 1,5 m height. Delineators were attached 0.5, 1.5 and 2.5 m above the snow surface at each location. The pine trees were about 3 m high. Distance at which delineators and pine trees were recognized at each location on different levels is shown in Figure 42 for several visual ranges(19).

8. CONCLUSIONS

Visual range is reduced by airborne precipitation particles such as blowing snow, fog, falling snow, and vehicle-generated snow particles. The fluctuation of visual range varies spatially and temporally, and effects human visual acuity･

Besides blowing snow, snow clouds behind vehicles that reduce driver's visibility have become a new concern on highways. Even in calm weather, visibility is reduced by airborne snow particles in the wake of vehicles on highways. As the temperature drops, cohesion of snow particle decreases and they are easily blown up from the road surface. The threshold of vehicle-generated snow clouds is derived from our observations. The fall velocities of snow particles in vehicle-generated snow cloud are of the same order as the vertical component of vertical wind speed fluctuation. Therefore, the height of vehicle-generated snow cloud corresponds to the height of the vehicle.

Wide dynamic range and high frequency of visual range in blowing snow reduce vehicle speed on snowy or icy road surface. We can estimate the cause of reduced visibility by calculating the dynamic visibility fluctuation using a visibility sensor, and this information can be useful for highway authorities and drivers.

A new visibility measuring system using CCD video camera has been certified by a comparison with a transmissometer. This is the only system that can measure visibility at six points simultaneously from one view point with real time scenery･

9. ACKNOWLEDGEMENTS

The author would like to express his sincere thanks to Prof.K. Kikuchi, Meteorological Laboratory, Department of Geophysics, Faculty of Science, Hokkaido University, for his valuable discussion. And he also would like to express his thanks to Prof. T. Harimaya, Dr. H. Uyeda and Dr. Y, Asuma of the same laboratory for their valuable advice.

And thanks are due to Dr. N4. Takeuchi, the former head of the road division of the author's institute, now, Hokkaido Branch, Japan Weather Association, for his continuous encouragements, valuable suggestions and for providing the author a chance to participate in the field of visibility attenuation related to transportation. Field observations have been supported by Mr. Y. Fukuzawa and other colleagues in the author's laboratory.

10. REFERENCES

1) American Meteorological Society. Glossary of Meteorology (5th printing), 1989, pp.613.

2)W.E.Knowles Middleton. Vision through the Atmosphere, 1968, University of Toronto Press.

3) M, Takeuchi. Investigation of Visibility in Snow Storm(in Japanese with English abstract), 1980, Hokkaido Development Bureau Civil Engineering Research Institute. Report No. 74. pp. 1-31.

4) K. Ishimoto and Y. Fukuzawa. Visibility in Blowing Snow Observed by the Luminance Contrast, 1985, Ann. Glaciol., Vol 6, pp.265-266.

5) Y. Fukuzawa, M. Takeuchi, and K. Ishimoto. Visibility Observed with a Reflector-Type Visibility Sensor(in Japanese), 1987, Abstract of Annual Meeting of the Hookaido district of the Japanese Society of Snow and Ice, pp.7.

6) M. Takeuchi. Vertical Profile and Horizontal Increase of Drift Snow Transport, 1 980, Journal of Glaciology, Vol.26, No, 94, pp.481 -492.

7) R.D. T abler. Using Visual Range Data for Highway Operations in Blowing Snow, 1 984, Optical Engineering Vol.23, No.l,PP.55-61.

8) M. Takeuchi, K. Ishimoto, and Y. Kajiya. Blowing Snow Problems and Their Countermeasures in Hokkaido, Japan. 1990, Proc., PIARC International Winter Road Congress, pp.249-261.

9) S. Kinoshita, E. Akitaya, and K.Tanuma. Snow and Ice on Roads II, 1970, Low Temperature Science, Ser.A,28, pp.311-323.

10) K. Ishimoto, and M. Takeuchi. Mass Flux and Visibility Observed by Snow Particle Counter, 1984, Memoirs of National Institute of Polar Research, Special Issue No.34, Proc.,ofThe Sixth symposium on Polar Meteorology and Glaciology, pp.104-112.

11)K. Ishimoto. Observation of Blowing Snow by a Snow Particle Counter with a Real-Time Processor. 1991, Proc., Japan-U.S. Workshop on Snow Avalanche, Landslide, Debris Flow Prediction and Control, pp.57-65.

12)K. Ishimoto, Y, Fukuzawa, and M. Takeuchi. Visibility Reduction Caused by Snow Clouds on Highways. 1993, Transportation Research Record NO. 13 87, Transportation Research Board, NRC of US A・ pp.178-182.

13) Robert E, Eskridge, J. C. R. Hunt. Highway Modeling Part l: Prediction of Velocity and Turbulence Field in the Wake of Vehicles, 1 979, J, Appl. Met., Vol 1 8,No.4, pp.3 87-400.

14) Y. Wada, T. Ooyama, and S. Imai. [Kankaku,Chikaku shinrigaku handbook] Handbook on Sense and Feeling in Psychology, 1979, Seishin shobou Corp., pp.15-16

15) K.Ishimoto, and M. Takeuchi, S. Naitou, and H. Furusawa. Development and Certification of A Visibility-Range Monitor by Image Processing. 1 989, Ann. Glaciol・, Vol.13, pp. 117-119.

16) K.Sadashige. An Overview of Solid-State Sensor Technology. 1987, SMPTE J・, pp.180-185.

17) MIkeda. Psychological Physics in the Sense of Sight (in Japanese). 1975, Morikita Publishing, p182.

18)K. Ishimoto, M. Takeuchi, Y. Fukuzawa, and T. Nohara. The Improvement of Reduced Visibility in Blowing Snow by Snow break Forest. 1980, Monthly Rep.of Civ.Eng.Res.Inst. No.320, pp. 17-25.

19) K. Ishimoto, Y. Fukuzawa. and M, Takeuchi. Visibility Reduction caused by snow and its countermeasures, 1994, Proc・,of Sth.PIARC International Winter Road Congress.

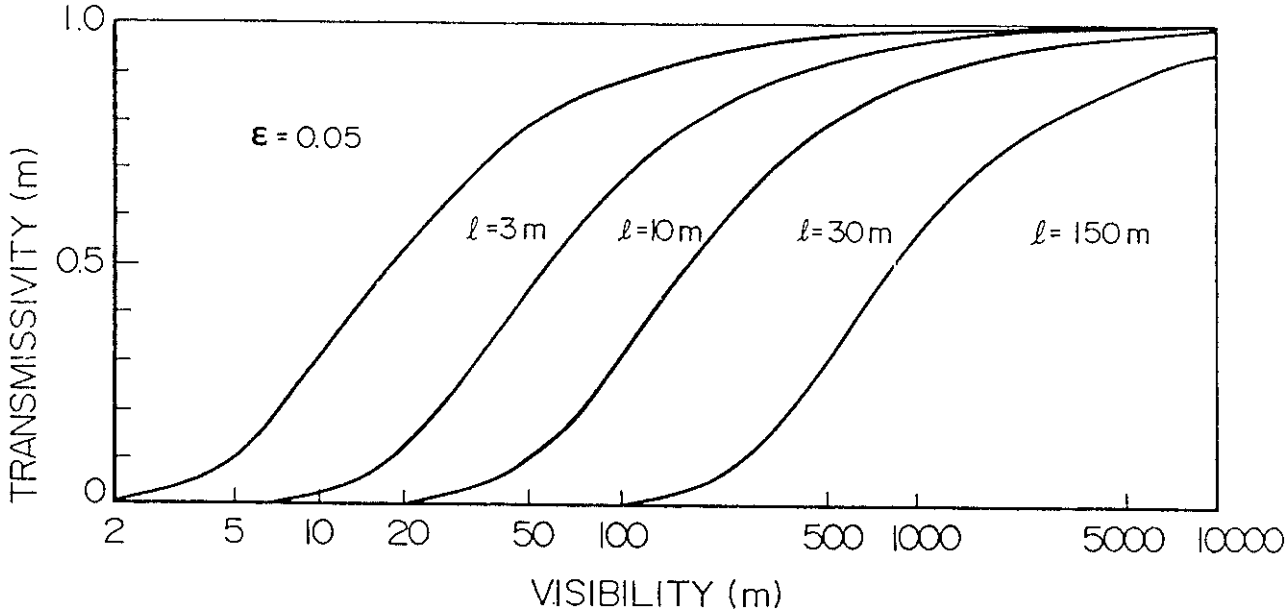

Figure 1 Visibility and transmissivity related to span of light

図－1　授受光間隔(1)に依存する視程と透過串の関係。精度良く測定できる視程は、授受光間隔に依存する。

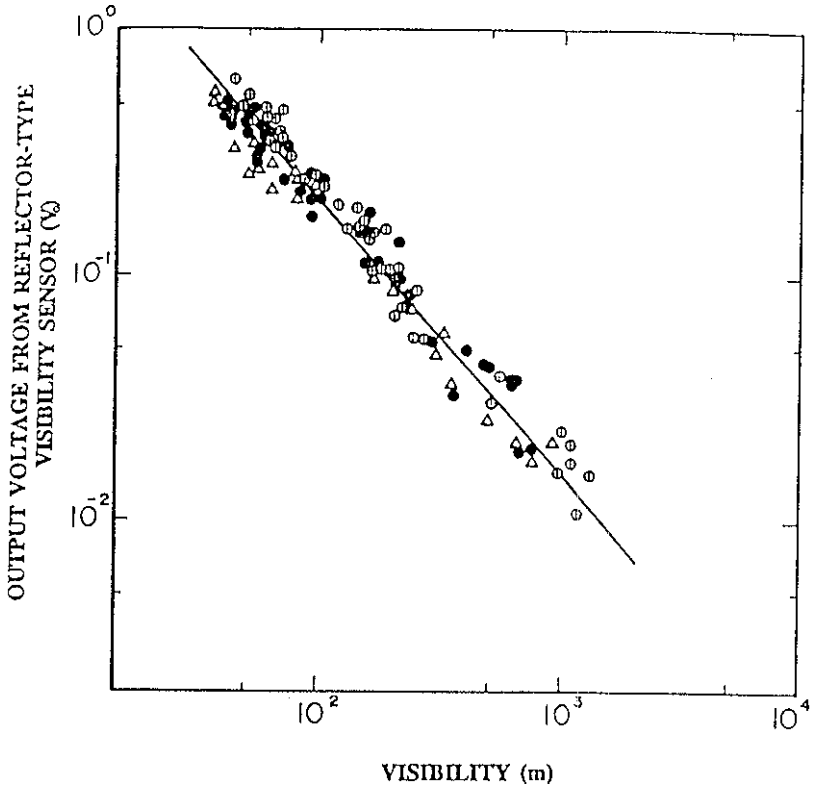

Figure 2 Output voltage of a reflector-type vlsibility meter and visibility by a transmissivlty

図－2　透過率型視程計による視程と反射型視程計の出力電圧

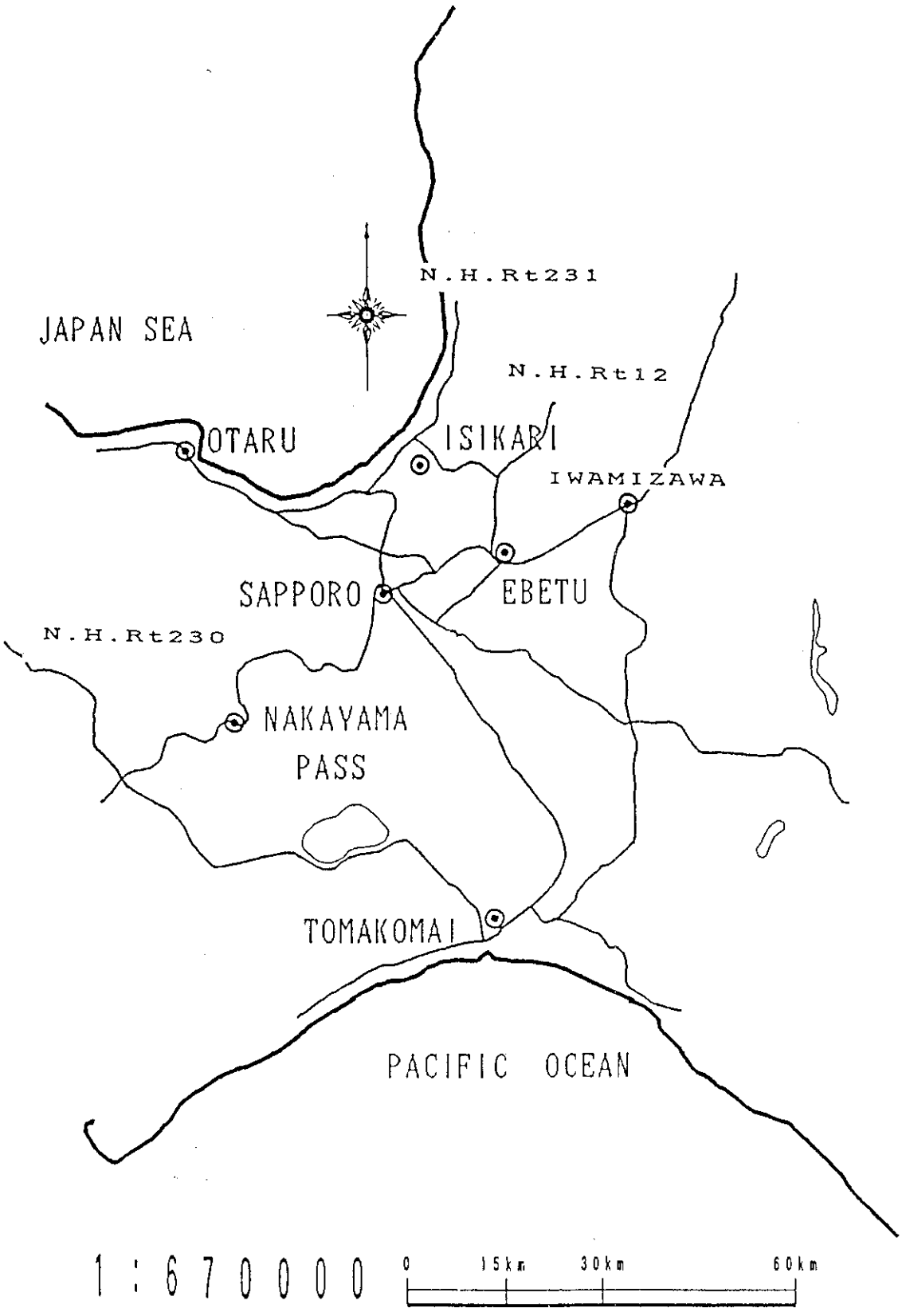

Figure 3 Main field observation points

図－3 主な観測地点

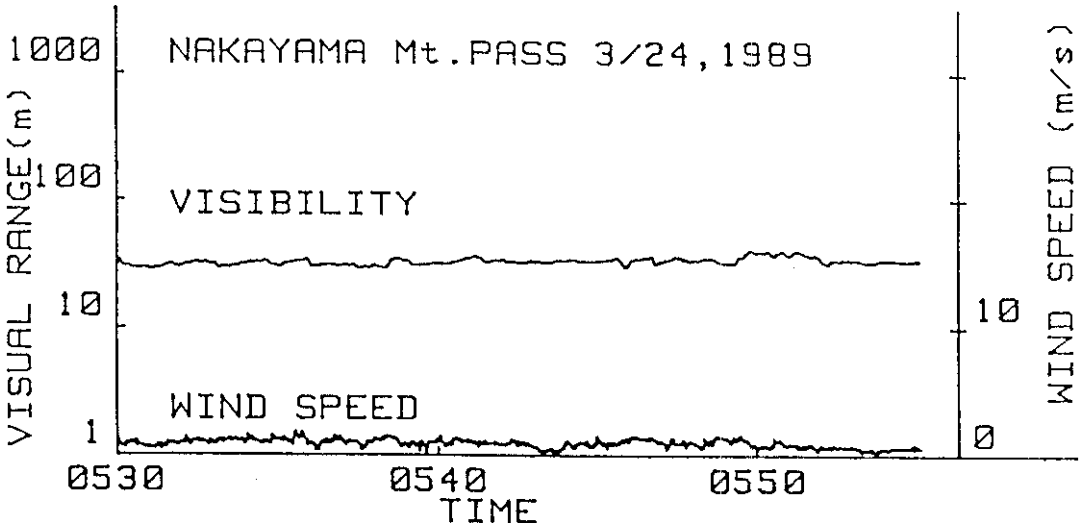

Figure 4 Visibility in fog on NHR 230 (Nakayama mountain pass)

図－４ 一般国道 230 号中山峠の霧発生時の視程

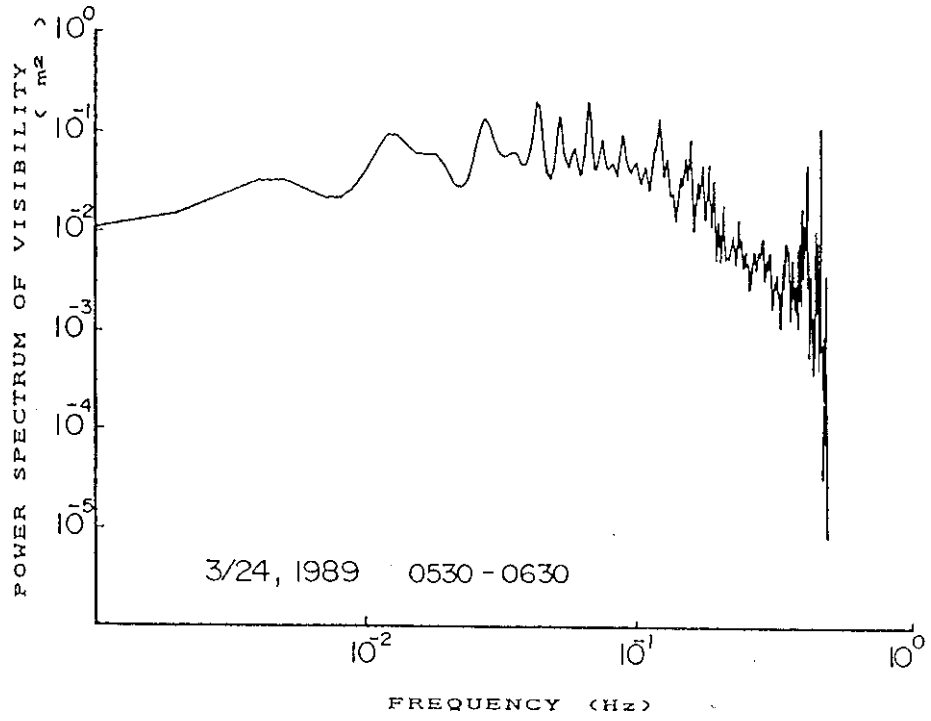

Figure 5 Power spectrum of visibility in fog

図－５ 霧発生時の視程変動スペクトル

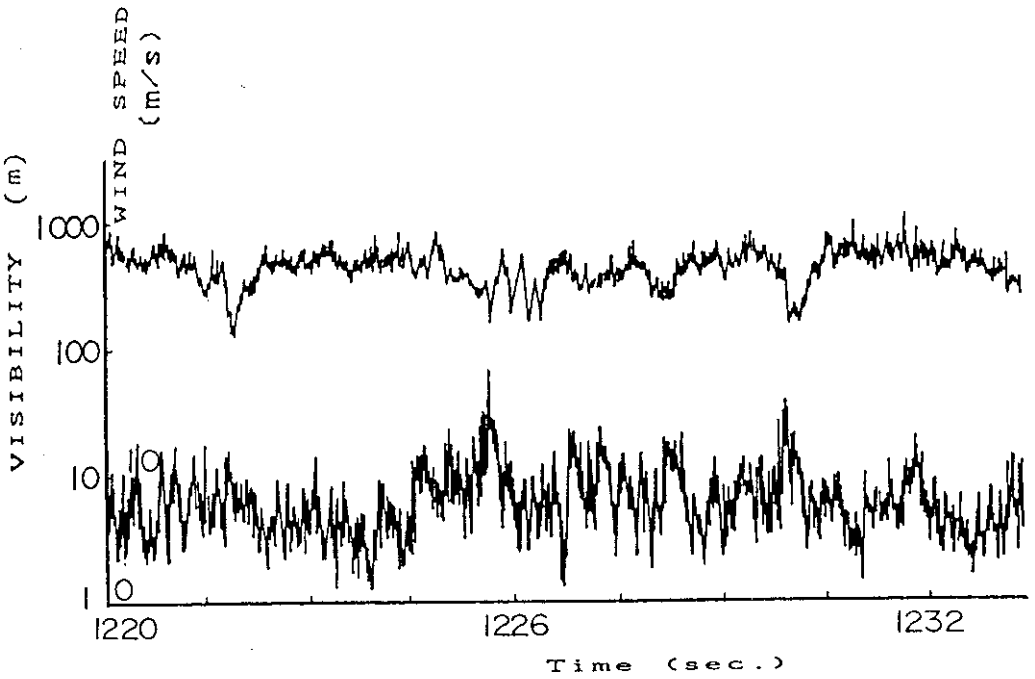

Figure 6 Visibility and wind speed in blowing snow at Nakayama mountain pass NHR 230

図－6　一般国道 230 号中山峠の吹雪時の視程変動

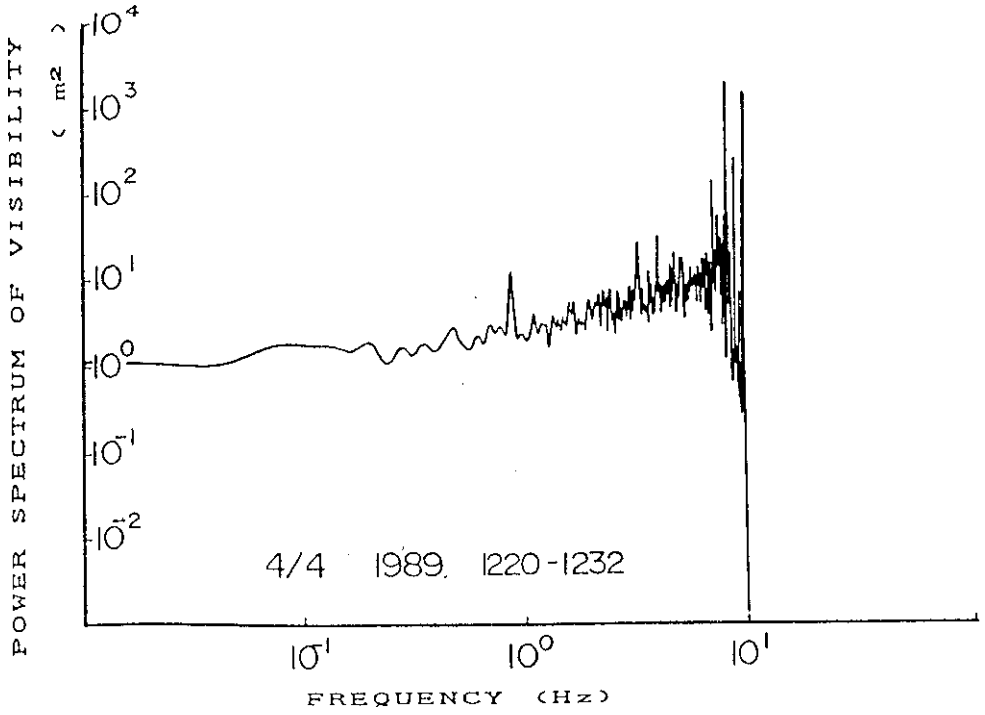

Figure 7 Power spectrum of visibility in blowing snow

図－7　吹雪発生時の視程変動スペクトル

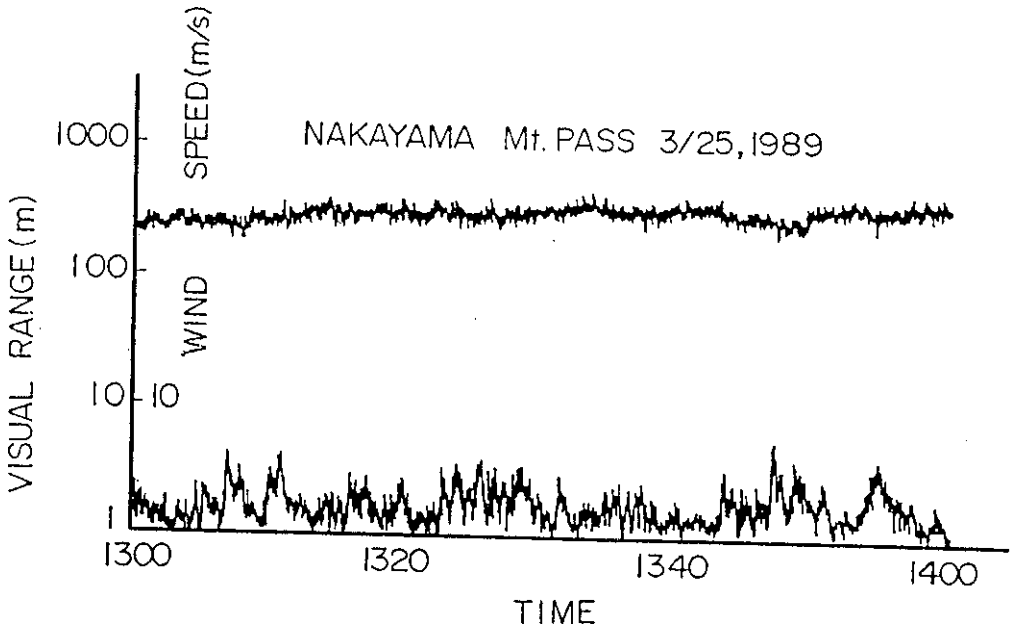

Figure 8 Visibility and wind speed in falling snow

図－8 降雪時の視程変動

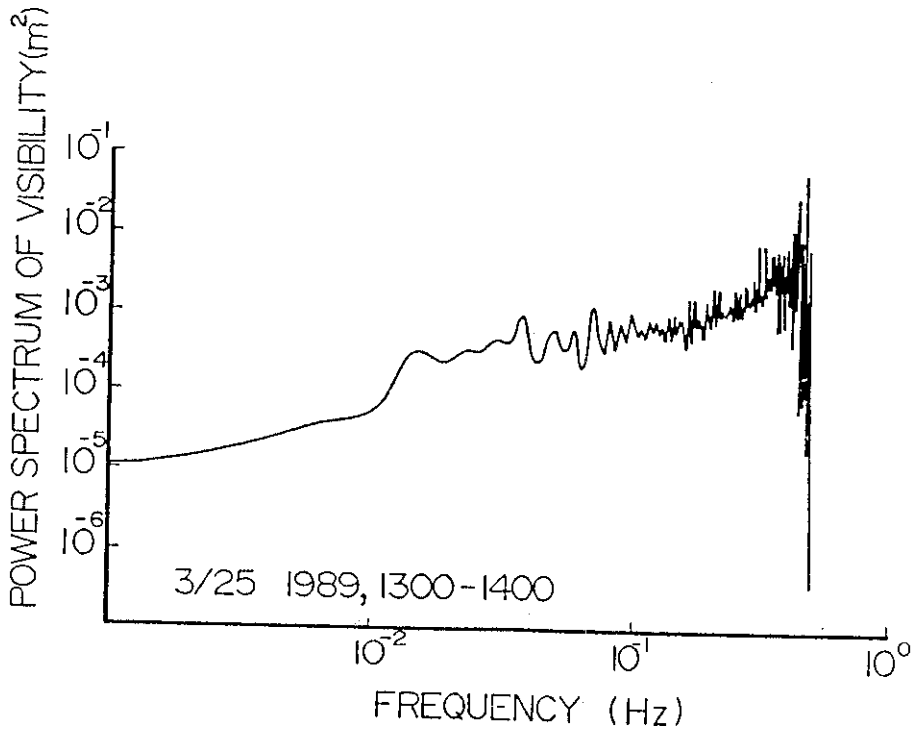

Figure 9 Power spectrum of visibility in falling snow

図－9 降雪時の視程変動スペクトル

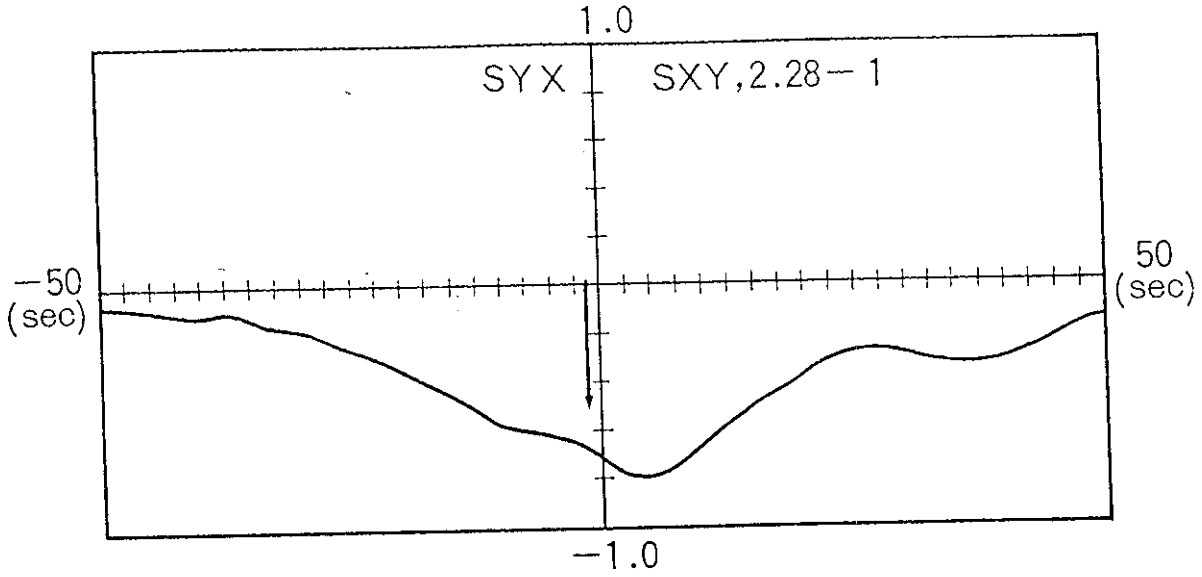

Figure 10 Cross－correlation between wind speed and visibility at 0.2 m above snow surface just after precipitation

図－10 降雪直後の雪面上 20cm における風と視程の相互相関
(下向き矢印が位置補正後の時間差ゼロの点、強風の数秒後に視程距離が短くなる変動をしている)

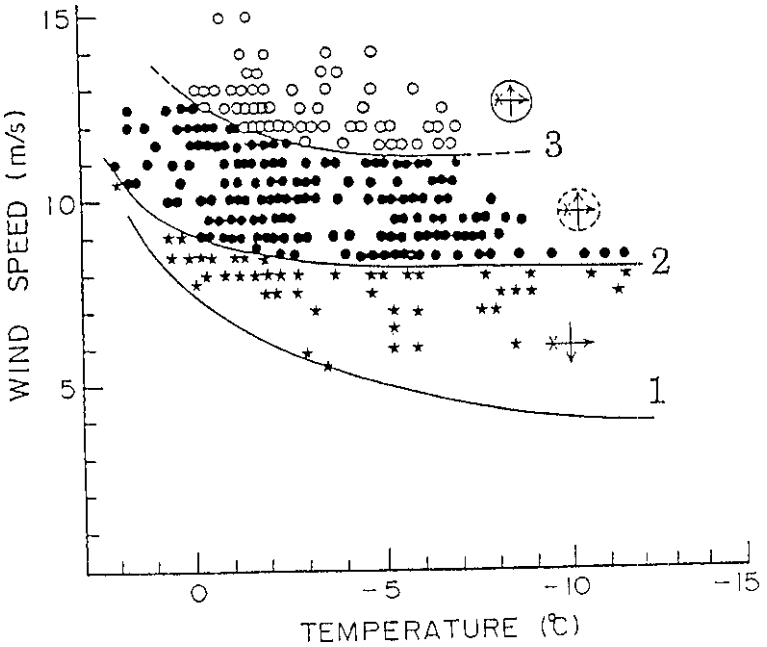

Figure 11 Threshold wind speed relating to temperature for saltation, curve 1, Intermittent threshold for suspension, curve 2, and for continuous suspension, curve 3

図－11 吹雪発生条件。曲線１：雪の跳躍運動発生条件、
２：間欠的に人の眼より高い吹雪が発生する条件、
３：連続的に高い吹雪が発生する条件

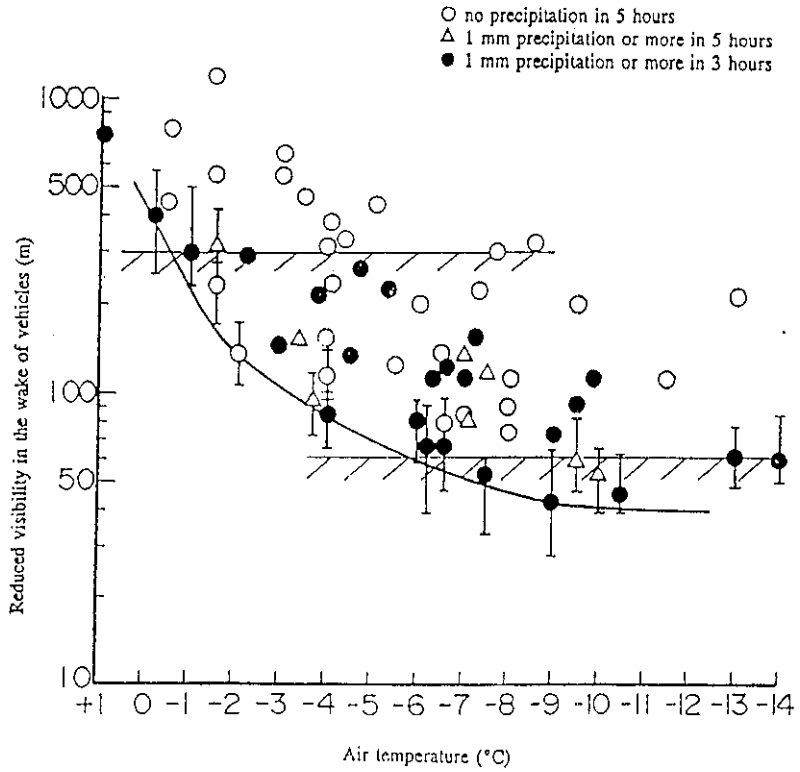

Figure 12 Threshold for reduced visibility by vehicle - generated snow cloud

図－12 大型車により雪煙が発生する条件

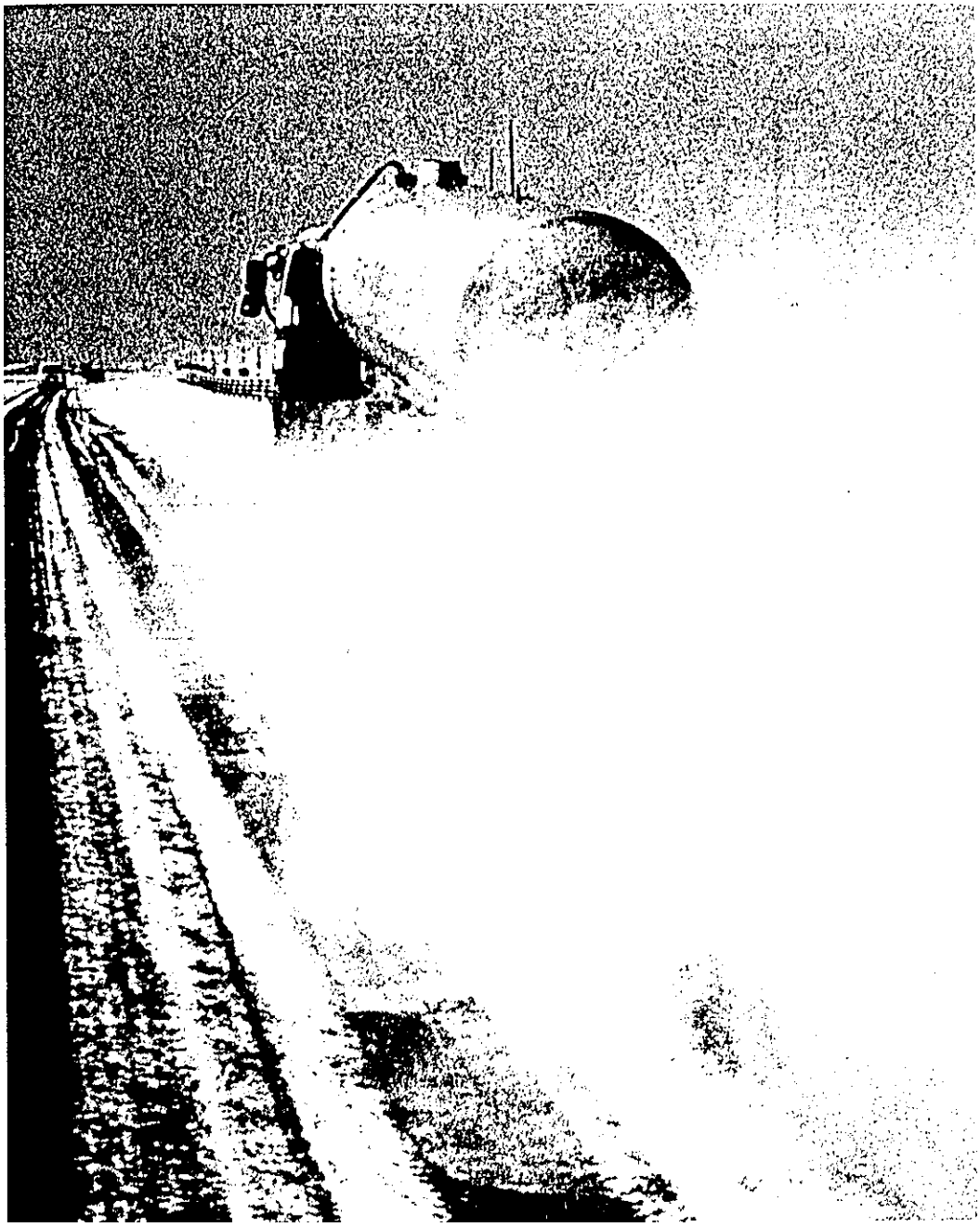

Figure 13 Snow Cloud generated by a large truck on the passing lane

図－13 追い越七車線を走行する大型車による雪煙発生状況

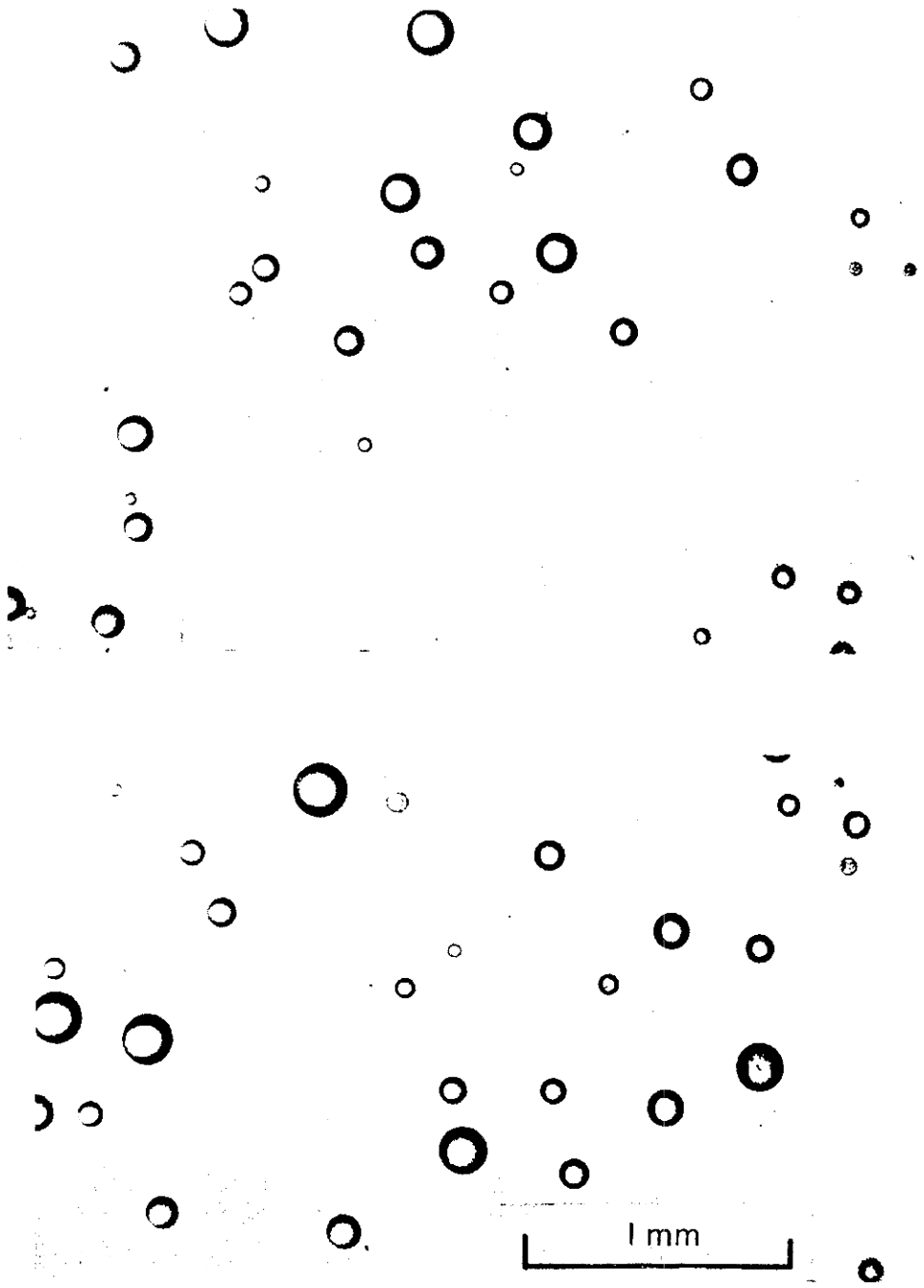

Figure 14 Melted snow particles on slide glasses covered with oil in blowing snow

図−14 ツェーダルオイルの上で融解した吹雪時の雪粒子

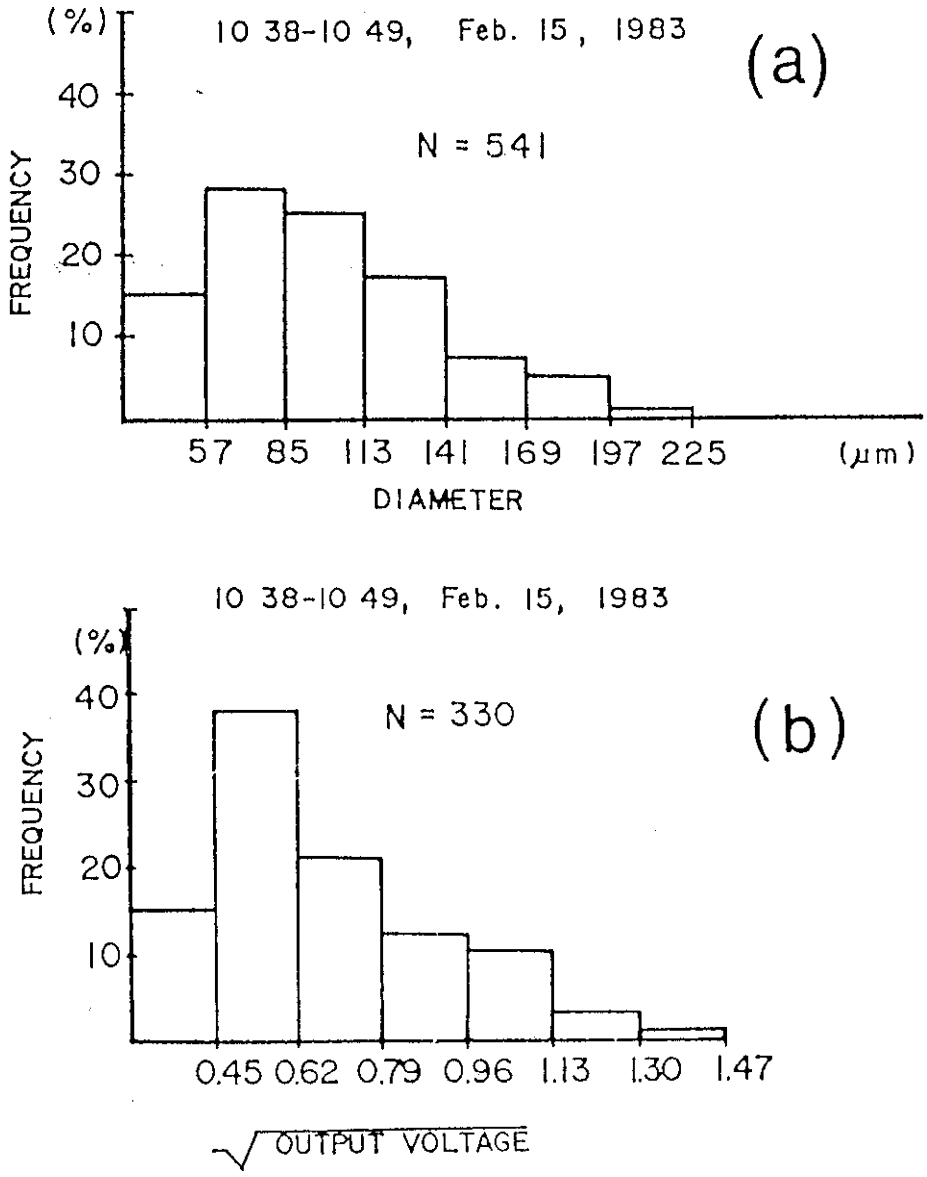

Figure 15 Distributions by snow particles by slide - glass method (a), and by a snow particle counter (b)

図－15 スノーパーティクルカウンター（ＳＰＣ）及び融解させた雪粒子から求めた吹雪時の雪粒子粒径分布の比較

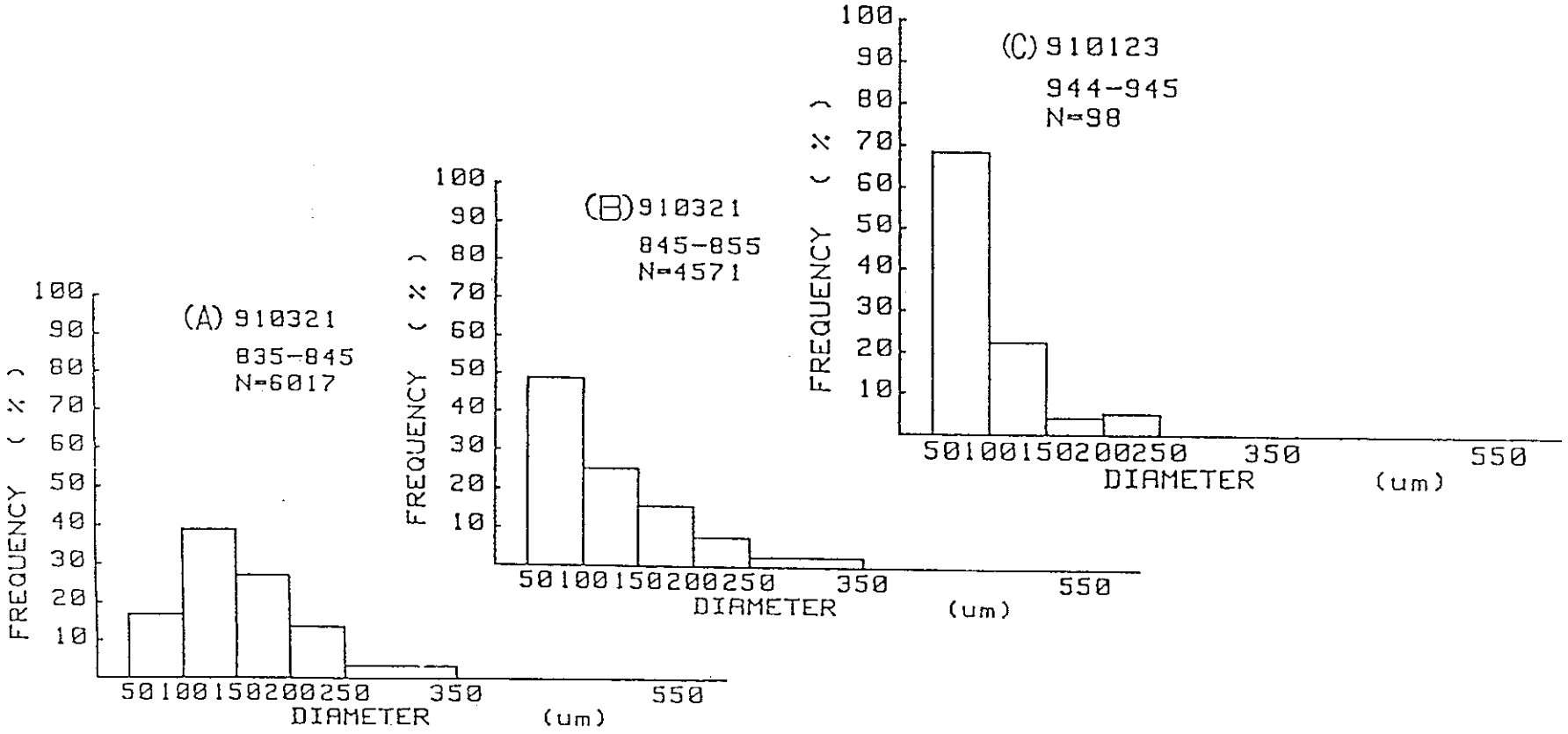

Figure 16 The size distributions of snow particles on a highway in blowing snow(A and B) and in vehicle-generated snow cloud(C)

図－16　ＳＰＣによる吹雪時（a、b）、雪煙発生時の雪粒子分布（c）

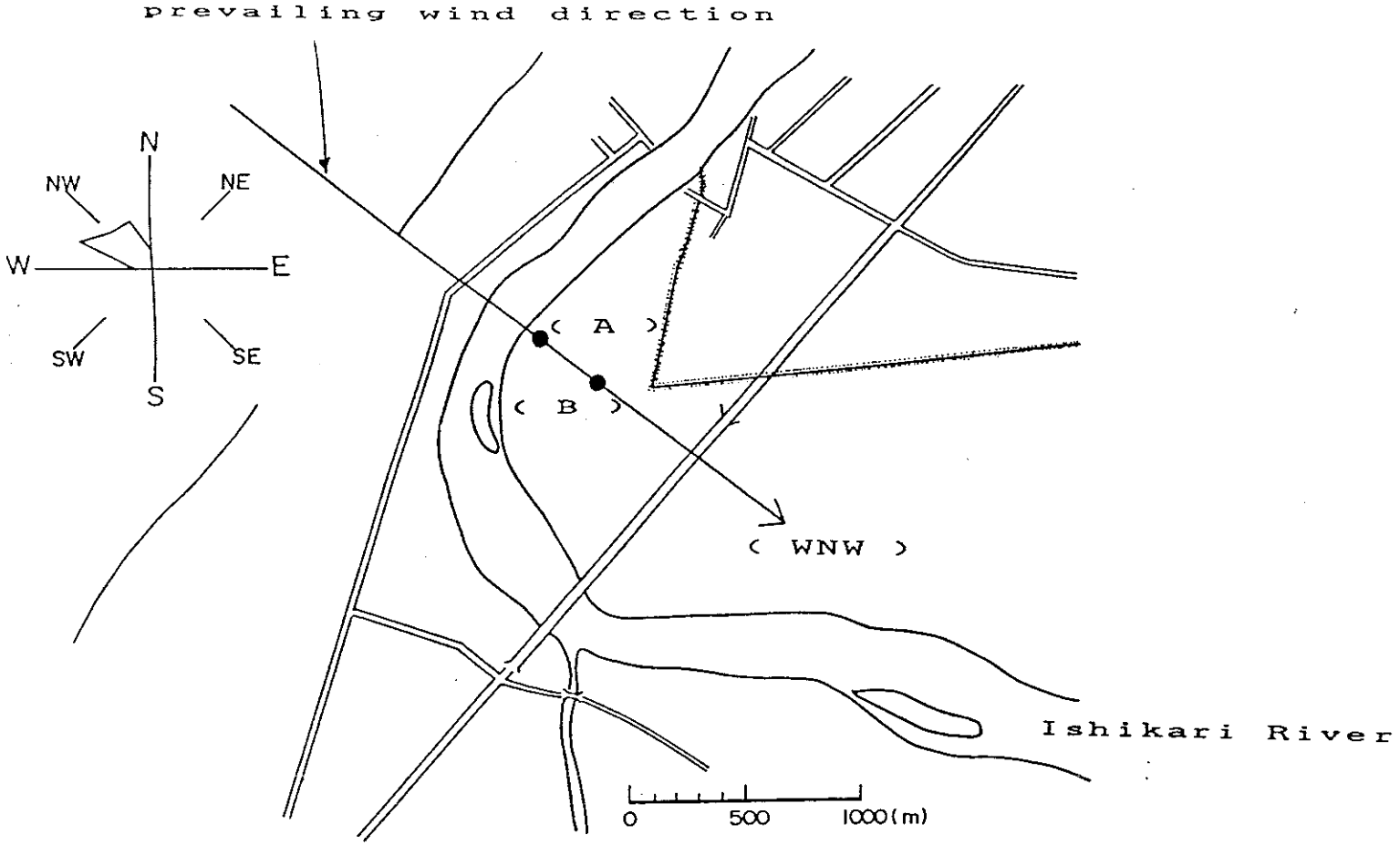

Figure 17 Observation point of surface fabric of snow cover in flooding area of Ishikari river (A, B: 10 and 300 m away from the edge of leeward flooding area)

図－17　石狩川右岸川岸から10m（A）、300m（B）離れた、主風向沿い、吹雪時の雪面雪粒子構造を観測した場所

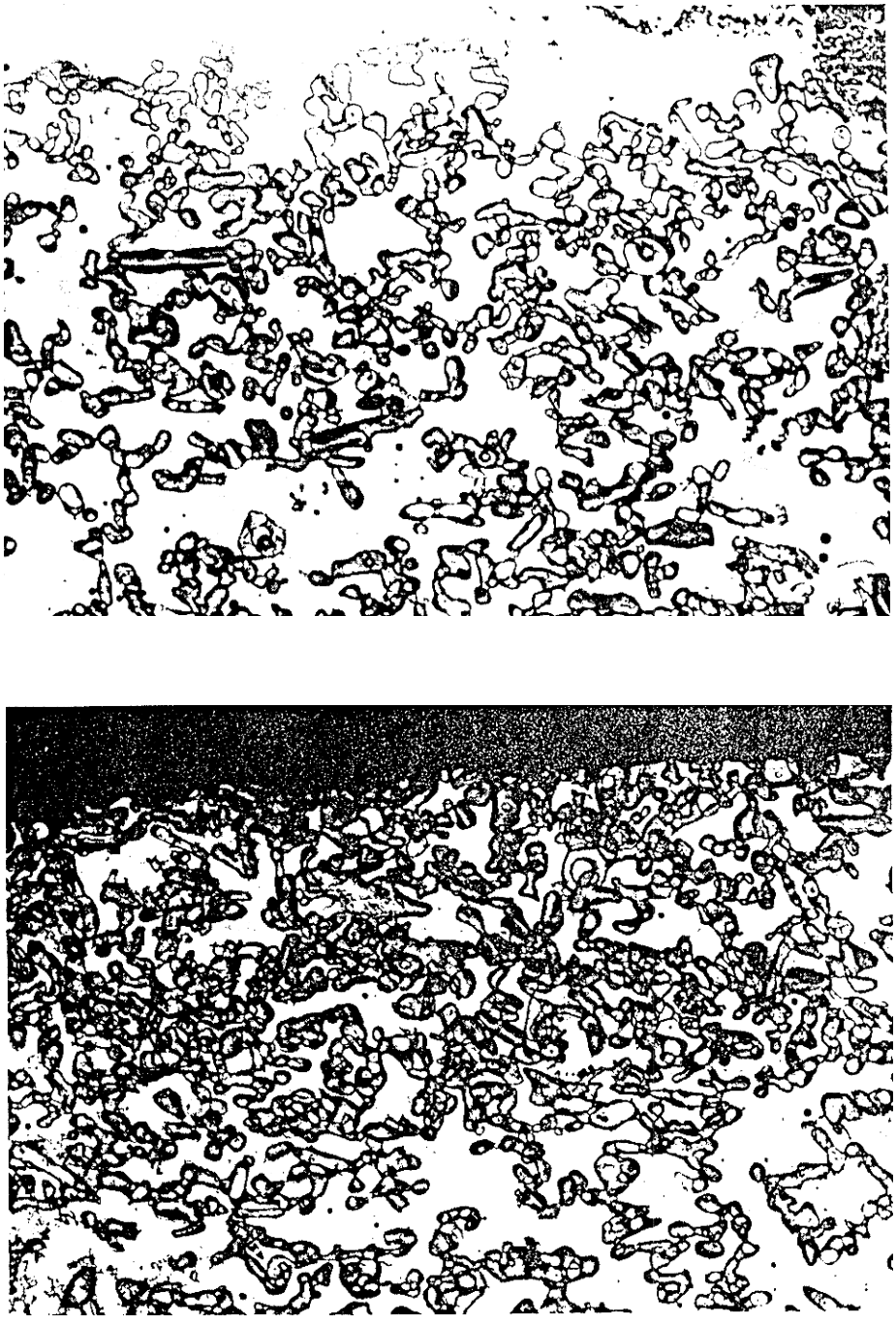

Figure 18 Thin sections of surface fabric of snow cover: (A) at the point of 10 m, (B) 300 m from the edge of leeward flooding area

図－18 積雪表面の薄片による雪粒子構造。A：川岸から10m（A)、B ： 300m （B）

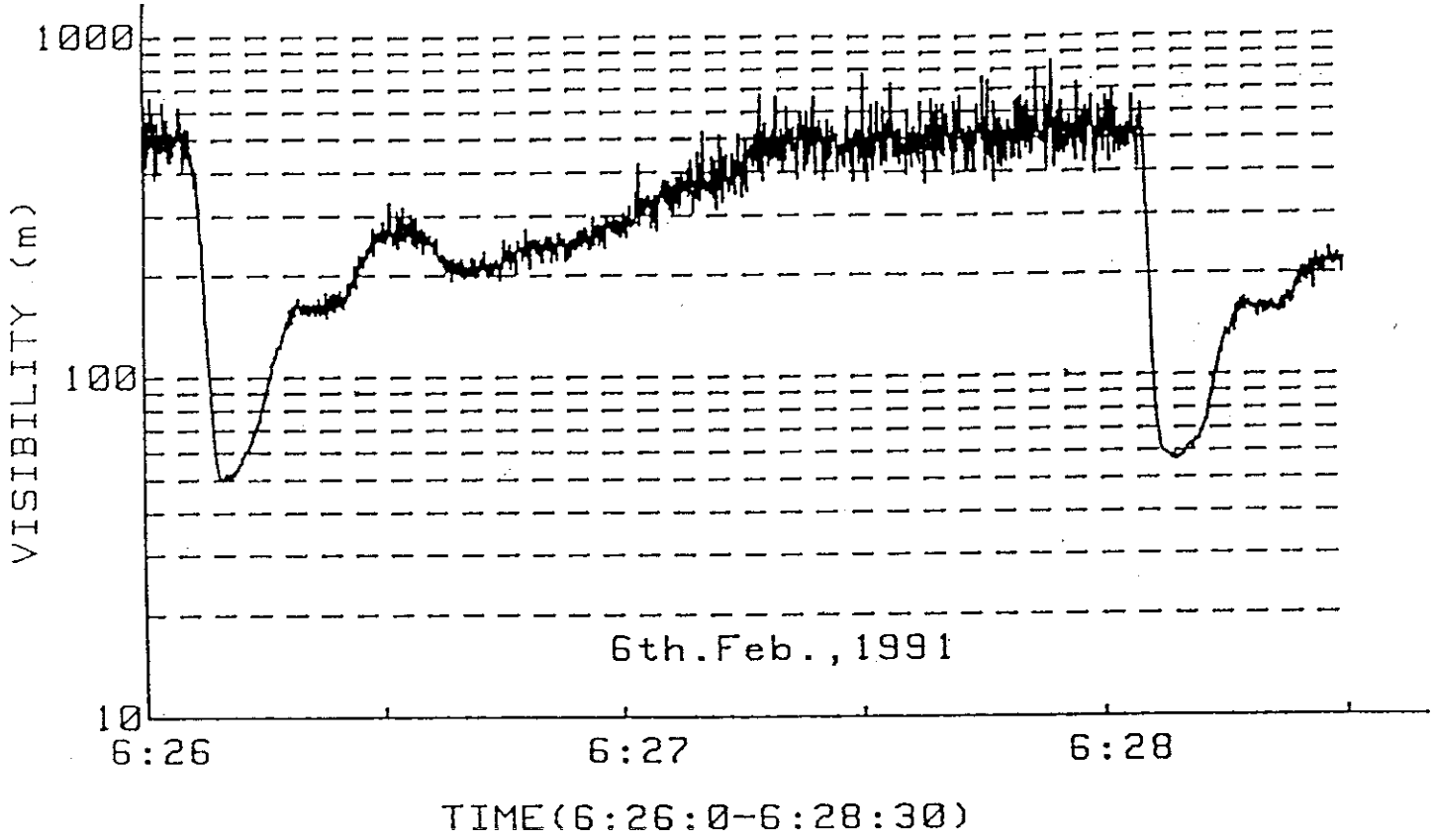

Figure 19 Reduced visibility by a large truck-generated snow cloud at Ebetu on NHR 12, measured by a reflector-type visibility meter set on the median on the road

図－19　一般国道12号江別太の中央分離帯に設置した反射型視程計で測定した、大型車による雪煙で減衰した視程距離。

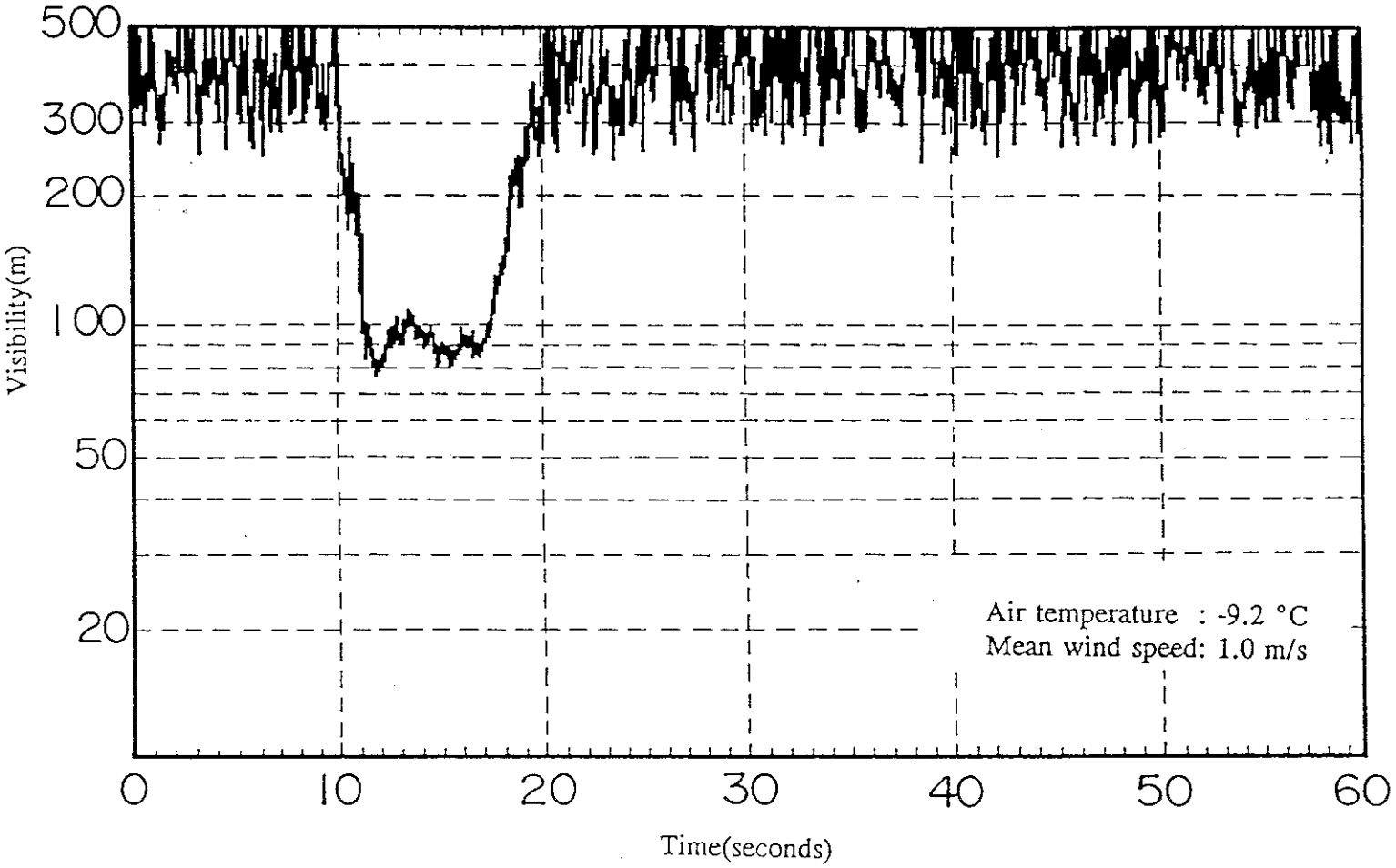

Figure 20 Reduced visibility by a large truck-generated snow cloud at Kaigen on NHR 40, measured by a reflector-type visibility meter set on the median on the road

図－20　一般国道40号の中央分離帯上の反射型視程計で測定された大型車による雪煙発生状況

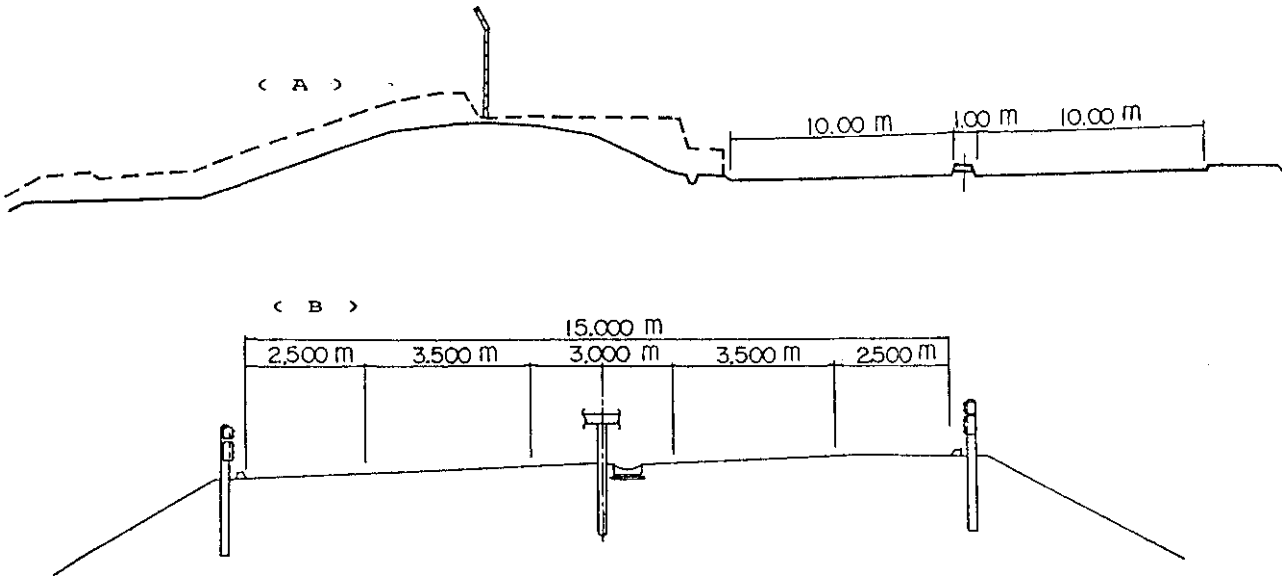

Figure 21 Cross sections at Ebetu, NHR 12 (A) and at Kaigen, NHR 40 (B)

図−21 道路断面図。一般国道12号（A)、40号（B）

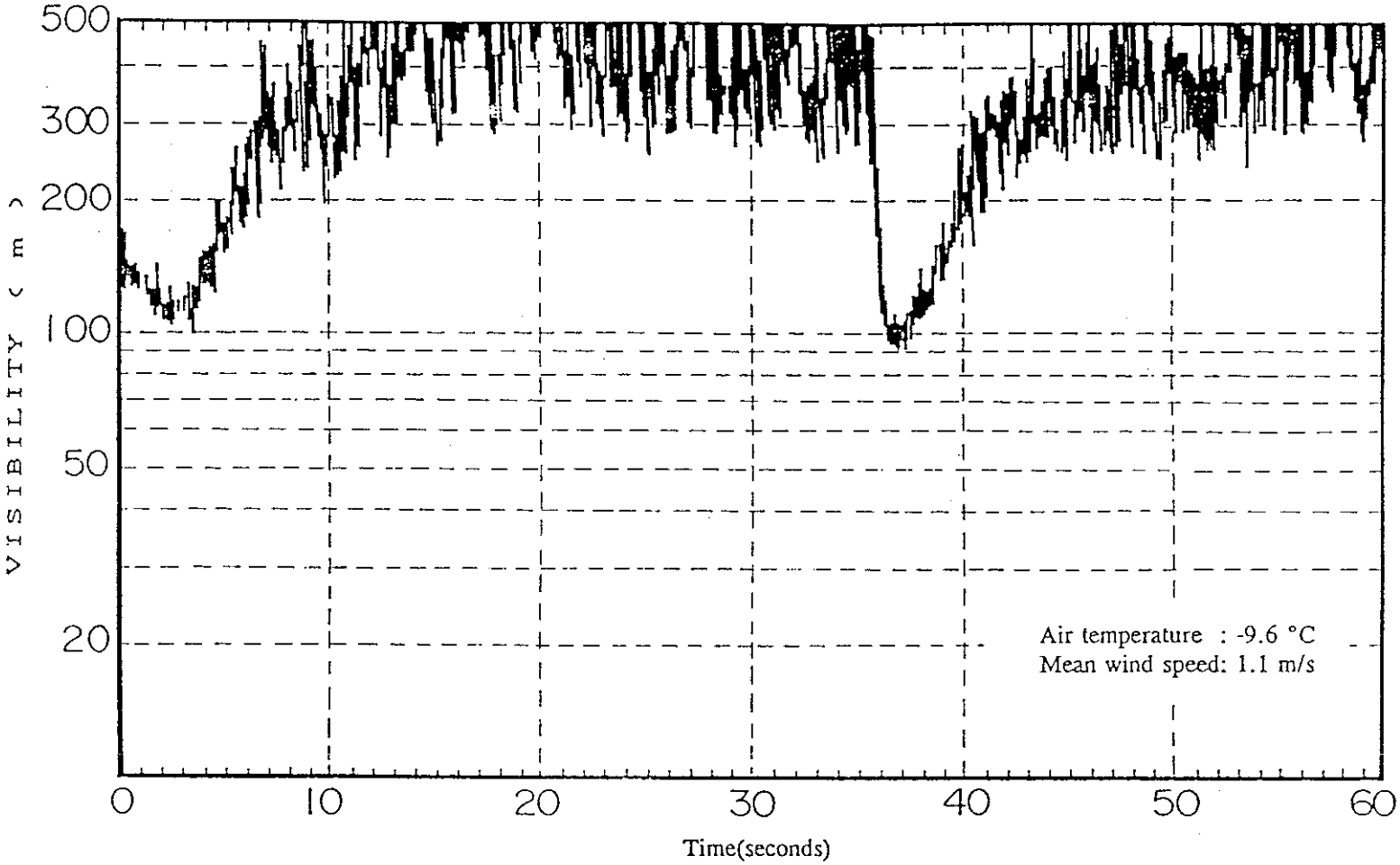

Figure 22 Reduced visibility by a small vehicle-generated snow cloud at Kaigen on NHR 40, measured by a reflector-type visibility meter set on the median on the road

図－22　一般国道40号の中央分離帯上の反射型視程計で測定された小型車による雪煙発生状況

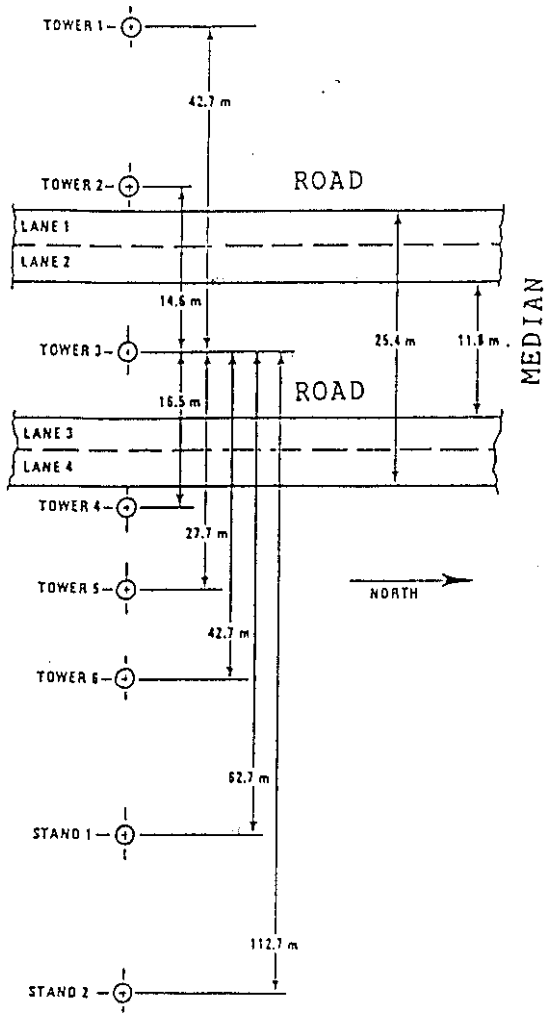

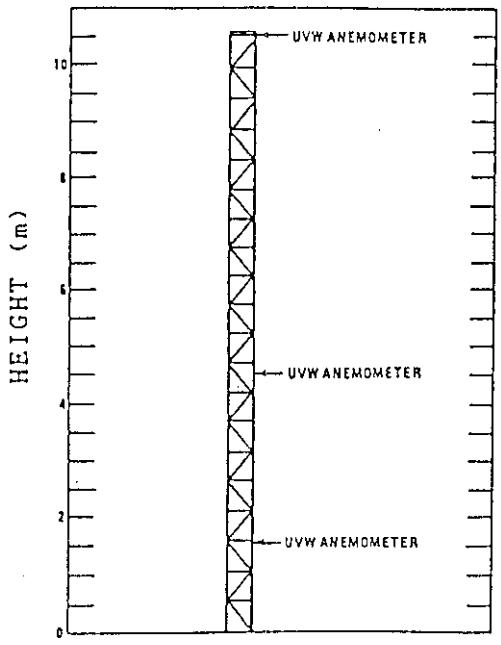

VERTICAL PROFILE OF TOWER 1～6

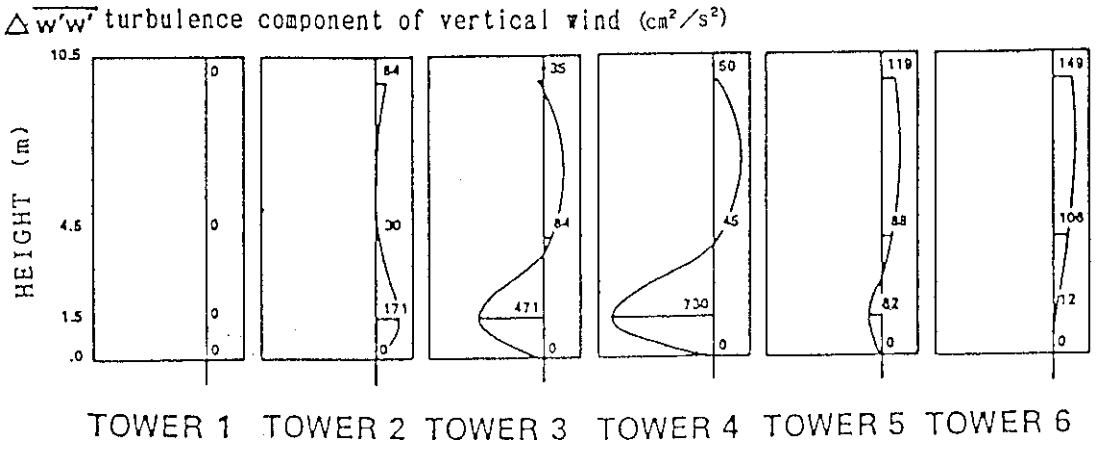

Figure 23 Vertical profile of wind fluctuation in vertical components (After Eskridge) 1979

図－23 風速変動の垂直分布

Figure 24 The height of vehicle - generated snow cloud

図－24　雪煙の高さ。およそ、大型車の車高程度であることがわかる。

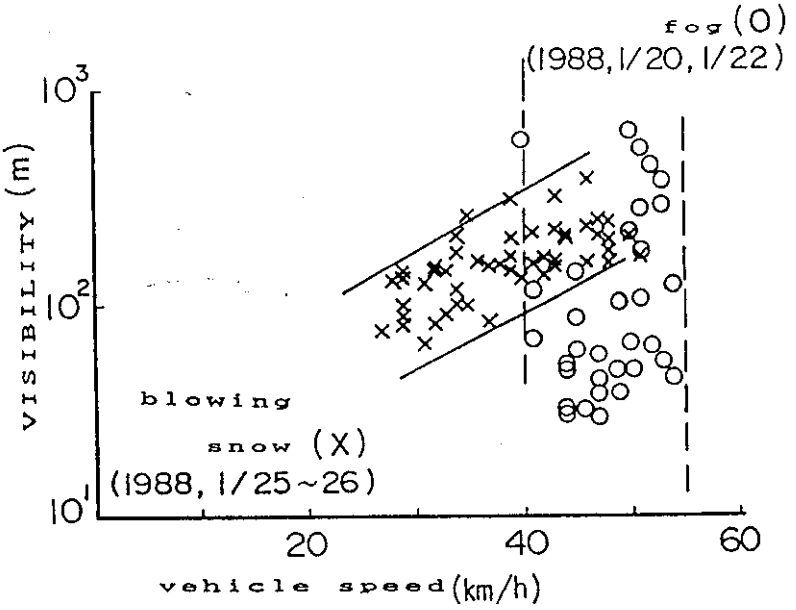

Figure 25 Vehicle speed to visibility averaged for 10 minutes in fog and in blowing snow wten road surface was covered with compacted snow and ice at Nakayama mountain pass on NHR 230 in January , 1988

図－25 路面が霊水状態の時、霧（○）と吹雪（×）による視程距離の減衰と車の速度。いずれも 10 分平均値(1988、1 月 25～26 日)。

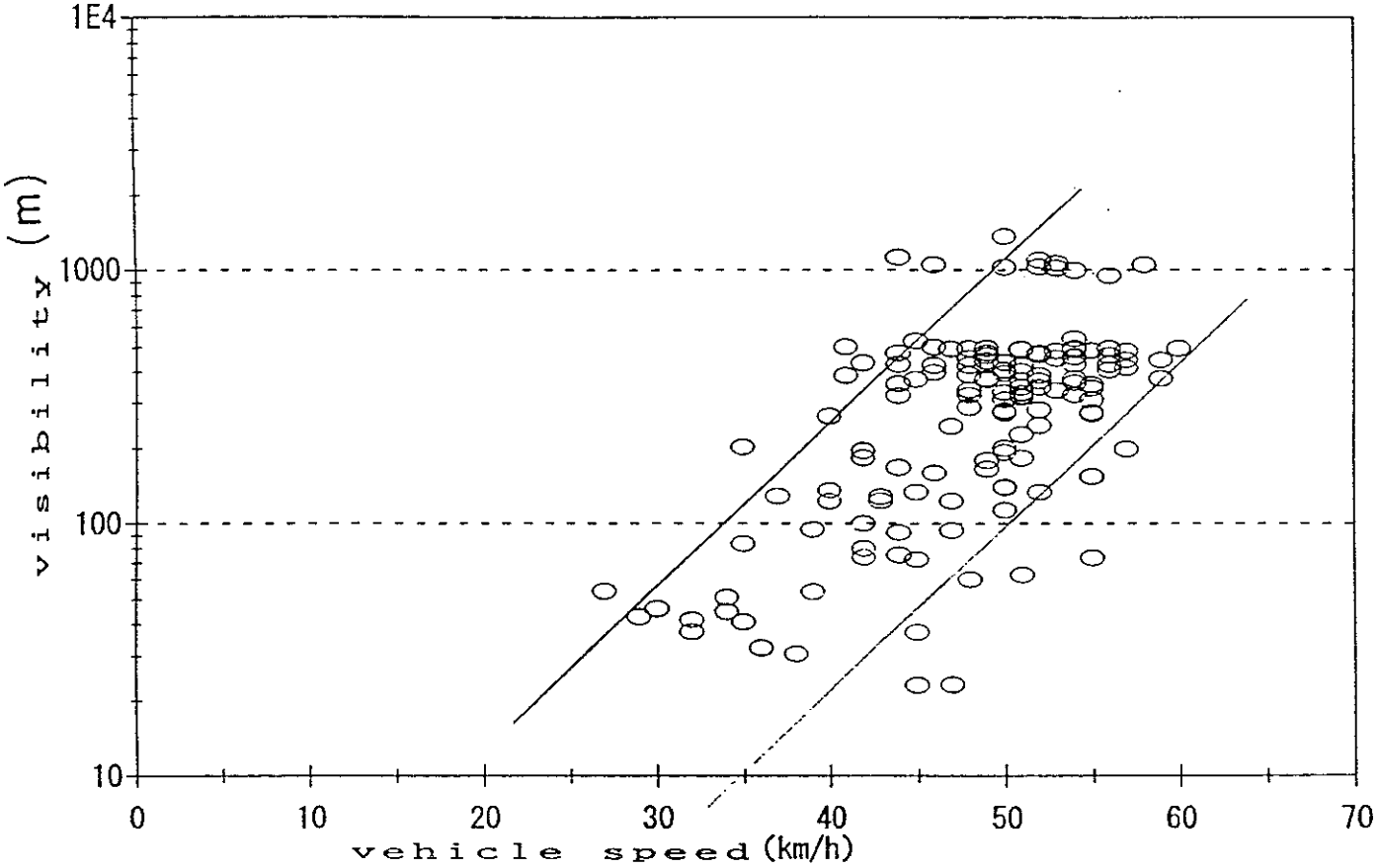

Figure 26 Vehicle speed to visibility averaged for 10 minutes in fog and in blowing snow when road surface was covered with compacted snow and ice at Nakayama mountain pass on NHR 230 when wind speed was over 8 m/s averaged for 10 minutes during January to March, and November to December in 1992

図－26　路面が雪氷状態の時、霧と吹雪による視程距離の減衰と車の速度の関係。いずれも10分平均値で、雪面からおよそ10mの高さの風速が10分平均値で８ｍ／ｓ以上の場合（一般国道230号中山峠。1992年１～３月、11～12月）。

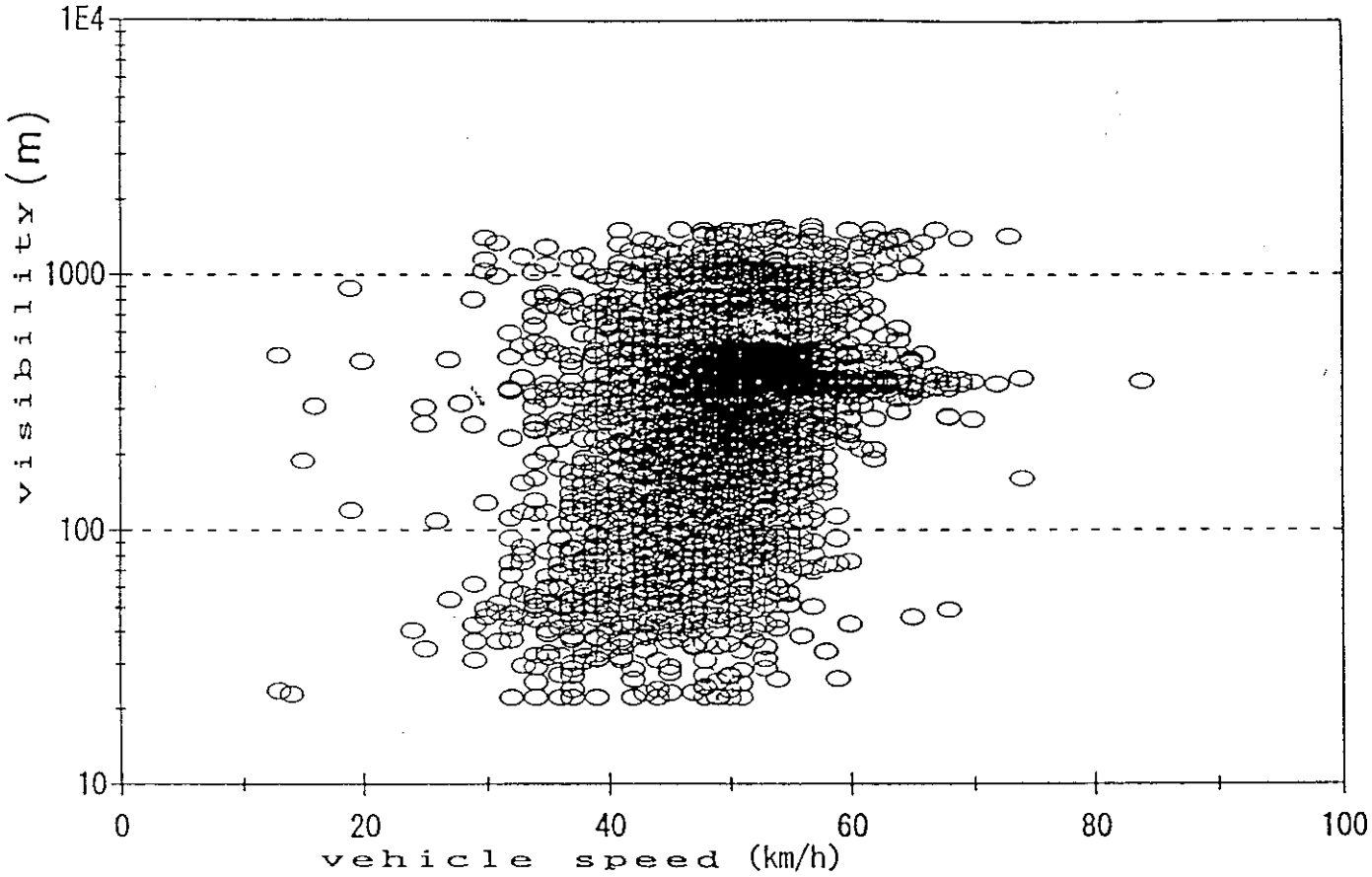

Figure 27 Vehicle speed to visibility averaged for 10 minutes in fog and in blowing snow when road surface was covered with compacted snow and ice at Nakayama mountain pass on NHR 230 when wind speed was under 8 m/s averaged for 10 minutes

図－27　路面が雪氷状態の時、霧と吹雪による視程距離の減衰と車の速度の関係。いずれも10分平均値で、雪面からおよそ10mの高さの風速が10分平均値で８ｍ／ｓ以下の場合（一般国道230号中山峠。1992年１～３月、11～12月）。

Table 1 Intensity of visibility fluctuation in various conditions calculated by equation (1), I and (2), IL

	blowing snow				falling snow	fog	snow cloud
mean vis.	40 m	71 m	305 m	604 m	297 m	32 m	516 m
I	40 %	55 %	66 %	35 %	14 %	12 %	65 %
IL	11 %	12 %	11 %	6 %	3 %	3 %	13 %

表－1 視程変動強度

$$I(\%) = \frac{\sqrt{\left(\overline{V}-V\right)^2}}{\overline{V}} \cdot 100$$

$$IL(\%) = \frac{\sqrt{\left(\overline{\log(V)}-\log(V)\right)^2}}{\overline{\log(V)}} \cdot 100$$

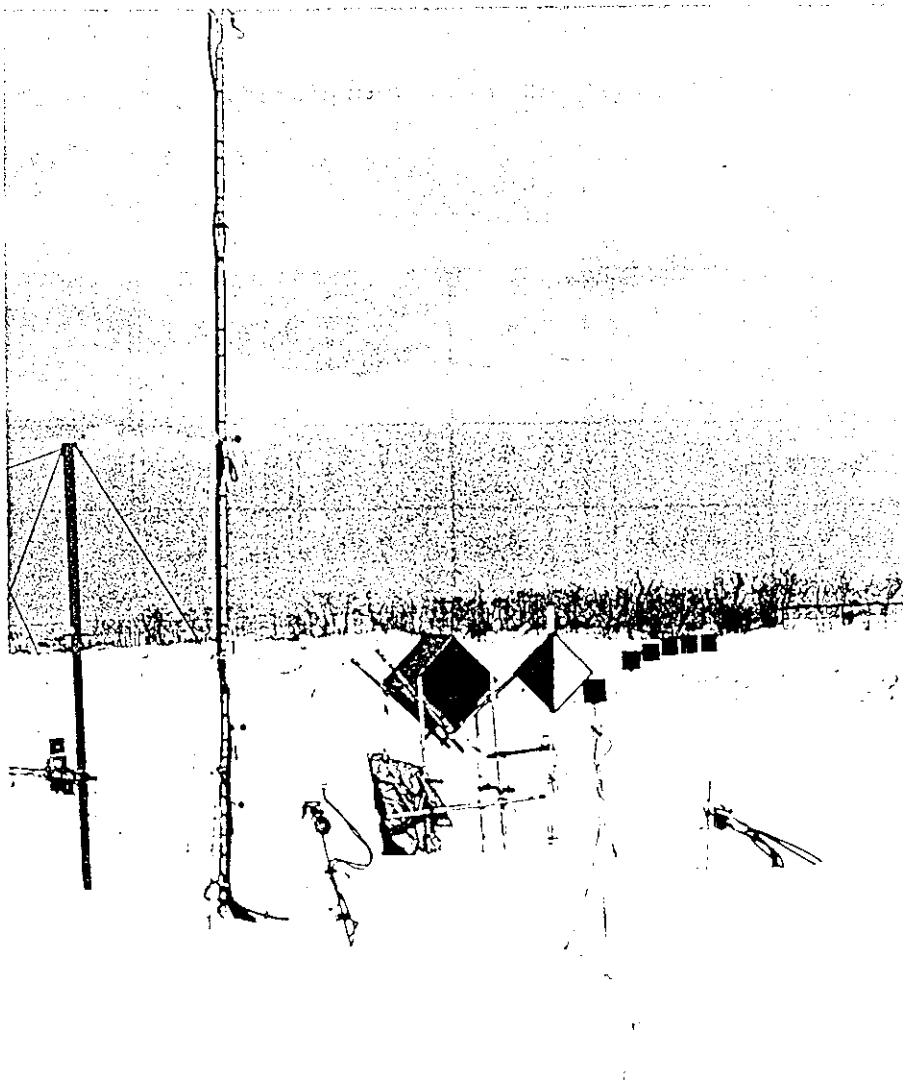

Figure 28 Black box for a luminance meter, the black and white target for a CCD camera and seven black target of a size equal to half the visual angle from the observation point

図－28 節度計による視程計測装置のための暗箱、ＣＣＤカメラのための白黒ターゲット、及び視角0.5度の視程板。

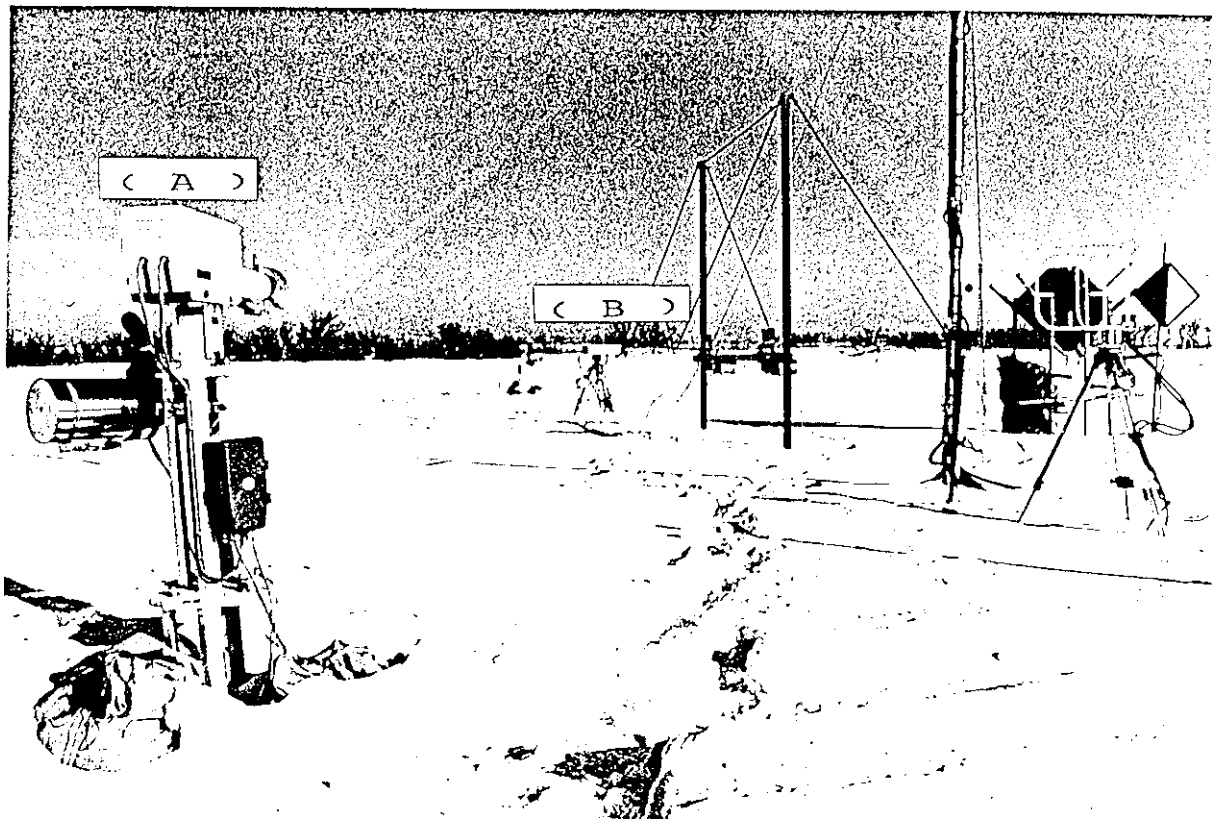

Figure 29 Transmissometer - type (A) and Reflector - type (B) visibility sensor

図－29 透過率型視程計（A）と反射型視計（B）

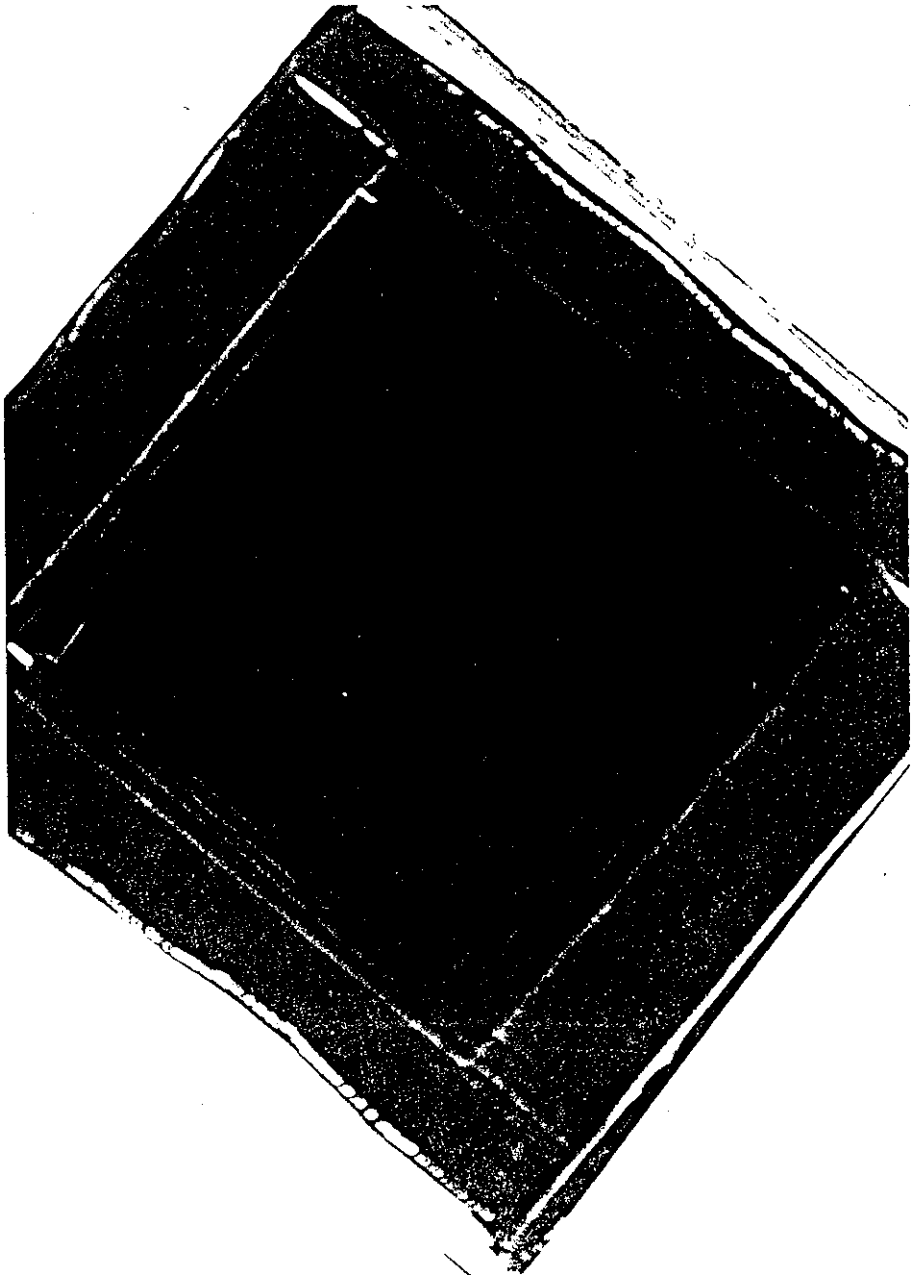

Figure 30 Black box with baffles to monitor the luminance without surrounding brightness

図－30 輝度計による視程計測装置のための暗箱。周囲の光を防ぐためスリットを入れて中心部がいつも極力暗くなるようにしてある。

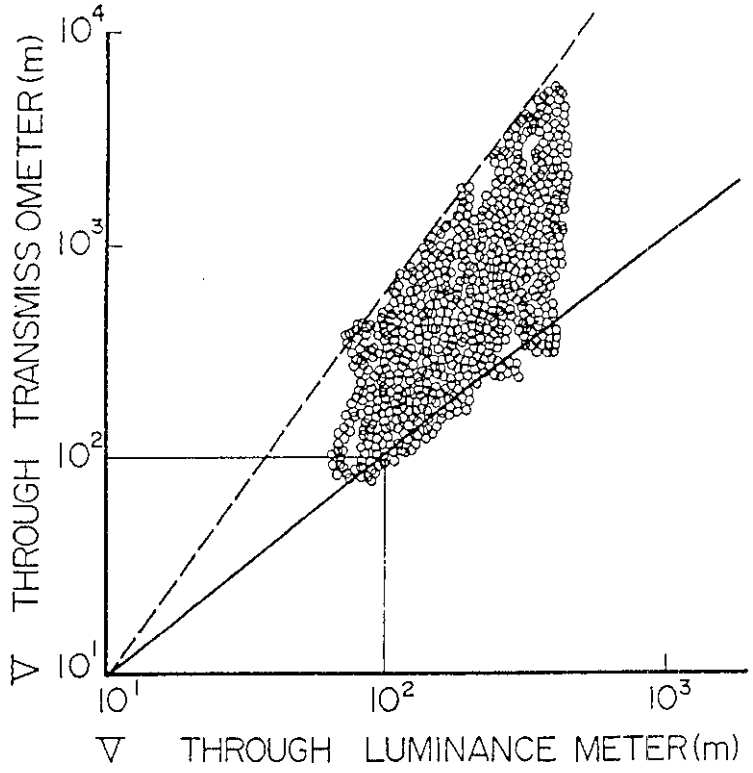

Figure 31 Visibility throuth luminance meter and through transmissometer

図−31 輝度計による視程（横軸）と透過率計による視程

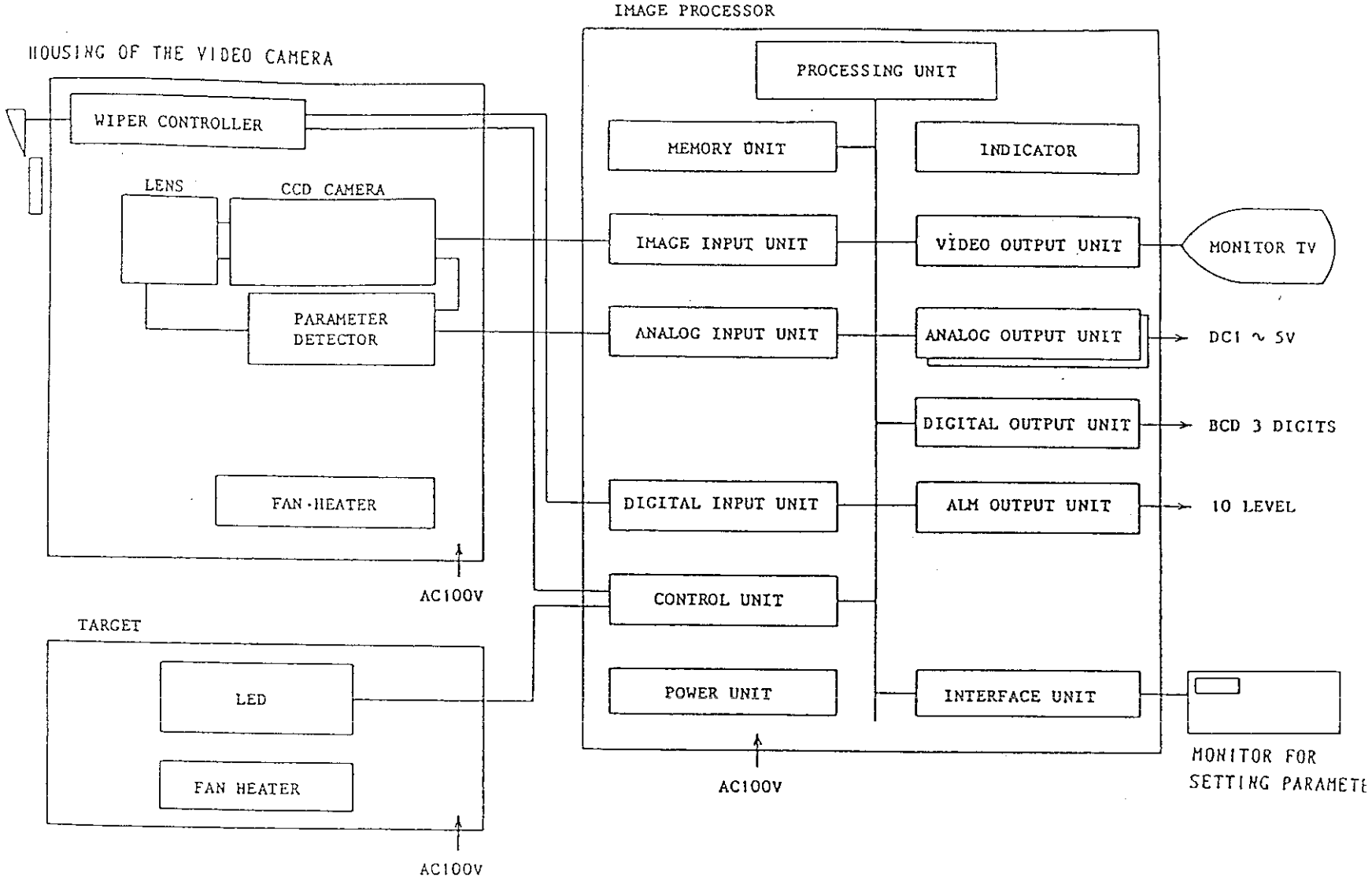

Figure 32 The block diagram of CCD visibility monitoring sy

図－32　ＣＣＤカメラによる視程計測システムのブロック図

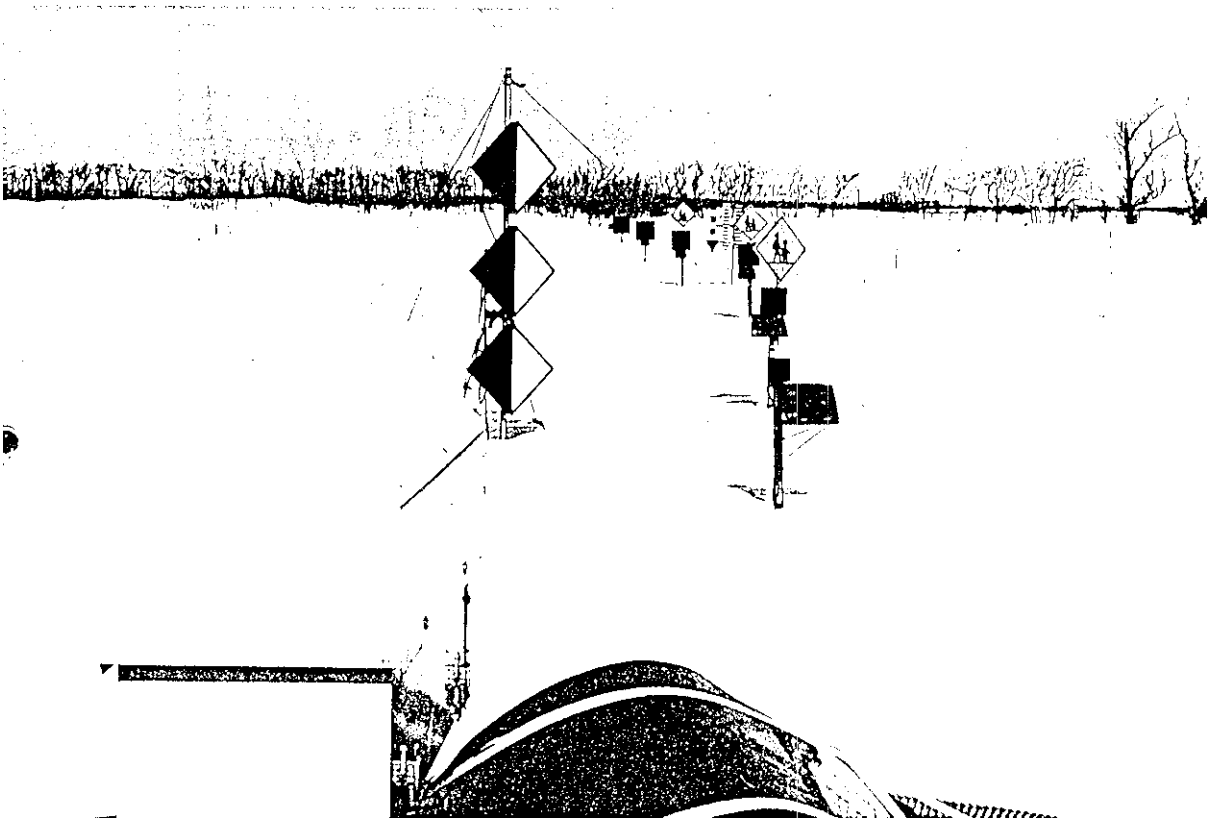

Figure 33 CCD video camera and three targets (0.45, 1.2 m respectively) above snow surface

図−33 ＣＣＤカメラを使った視程計測システム

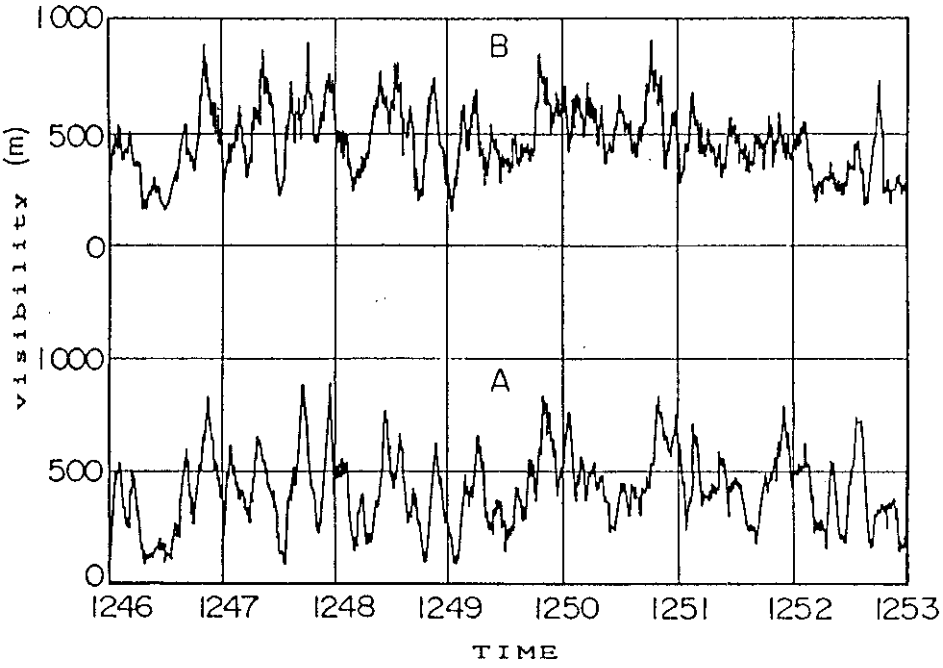

Figure 34 The trend of the visibility by the CCD video camera (A) and that by the transmissometer

図－34 視程の時間変動。ＣＣＤカメラ（A)、透過串型視程計（B）

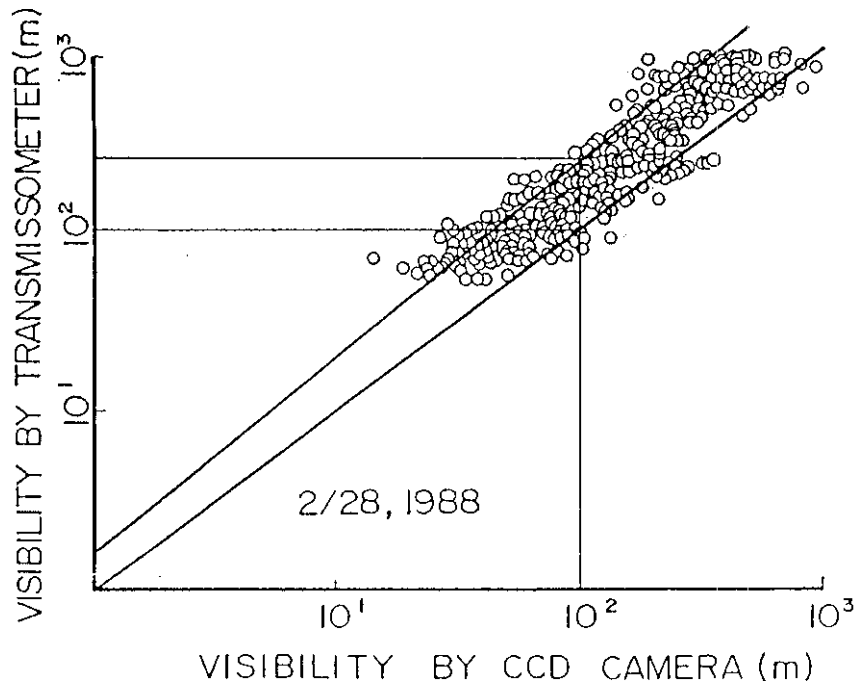

Figure 35 Visibility by a transmissometer and that by a CCD camera

図－35 ＣＣＤカメラ型視程計（横軸）と透過率型視程計（縦軸）

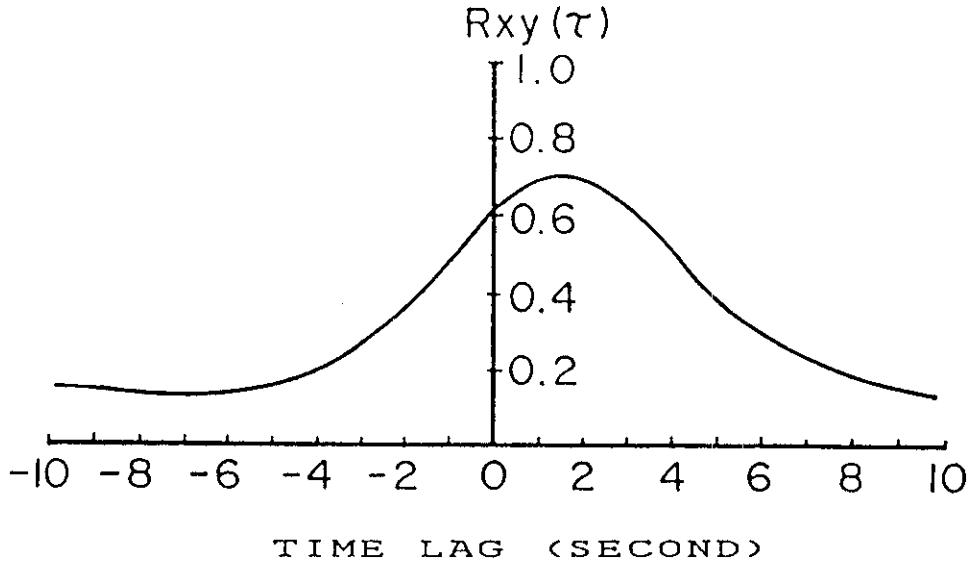

Figure 36 The cross - correlation coefficient between visibility at the point of the CCD camera and that at tHe point of the transmissometer

図－３６　ＣＣＤカメラ型視程計と透過率型視程計の相互相関関数。主風向沿いに位置がずれた分だけ相関のピーク値の時間がずれており、風速でこのずれが説明できる。

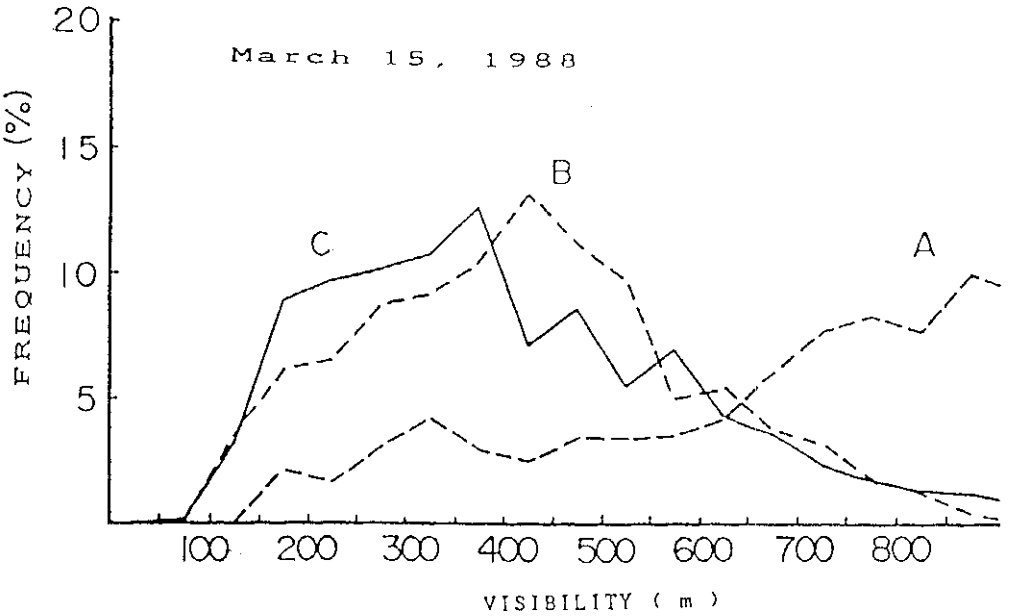

Figure 37 THe appearance frequency of poor visibility at three levels above snow surface (A : 2 m, B : 1 in , C : 0 . 4 5 m)

図－37　書面から４５ｃｍ（C)、１ｍ（B)、２ｍ（A）の高さでの視程距離減衰の頻度。雪面に近いほど視程距離が短い頻度が多い。

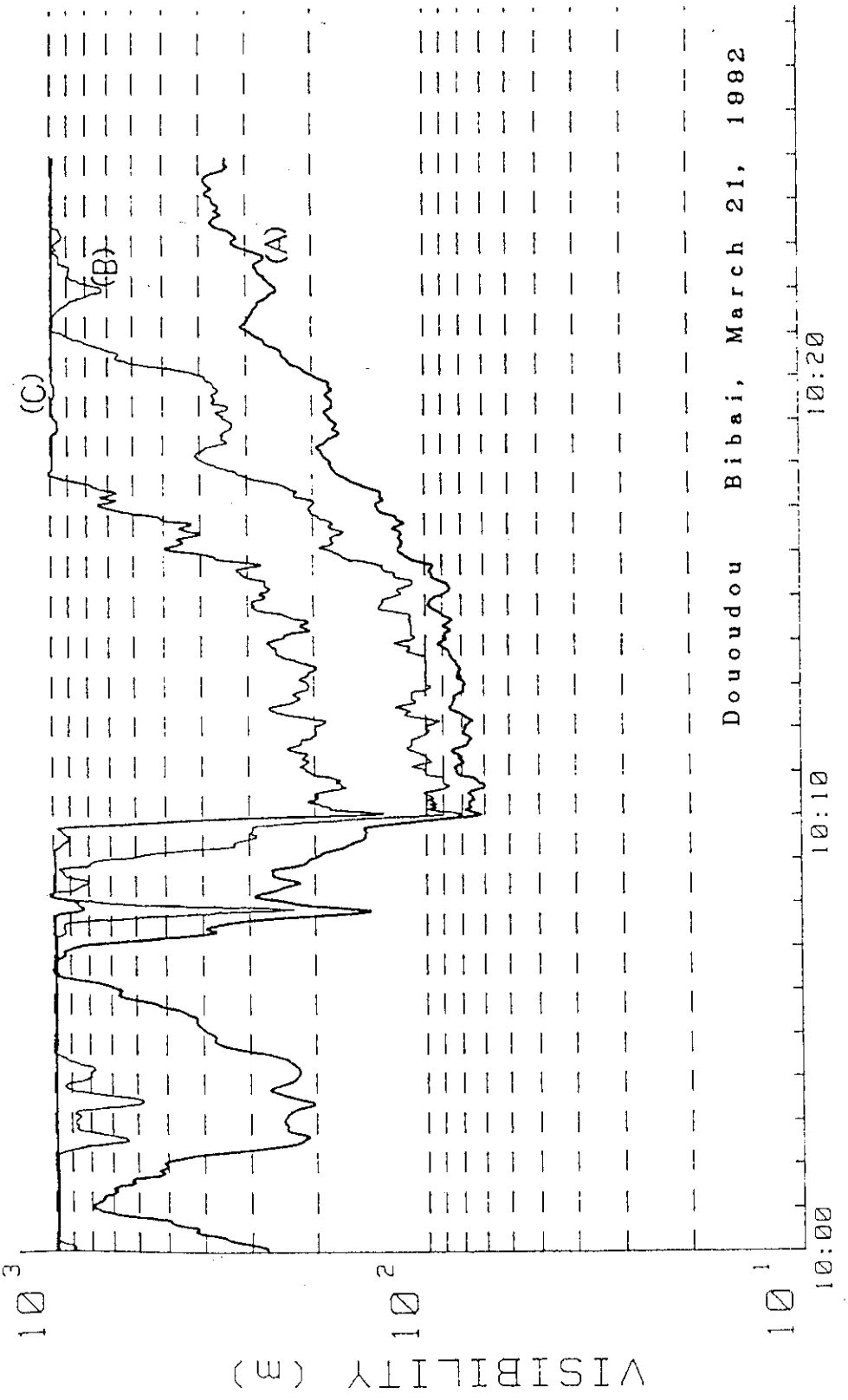

Figure 38 Visibility at three levels (A,B,C: 0.5, 1.5, 2.0 m) on the road side on Douou expressway from one view point at 1.5 m high along the road

図－38 盛土道路の路側の雪面上1.5mから観測した雪面上0.5, 1.5, 2 m (A、B、C) の視程変動

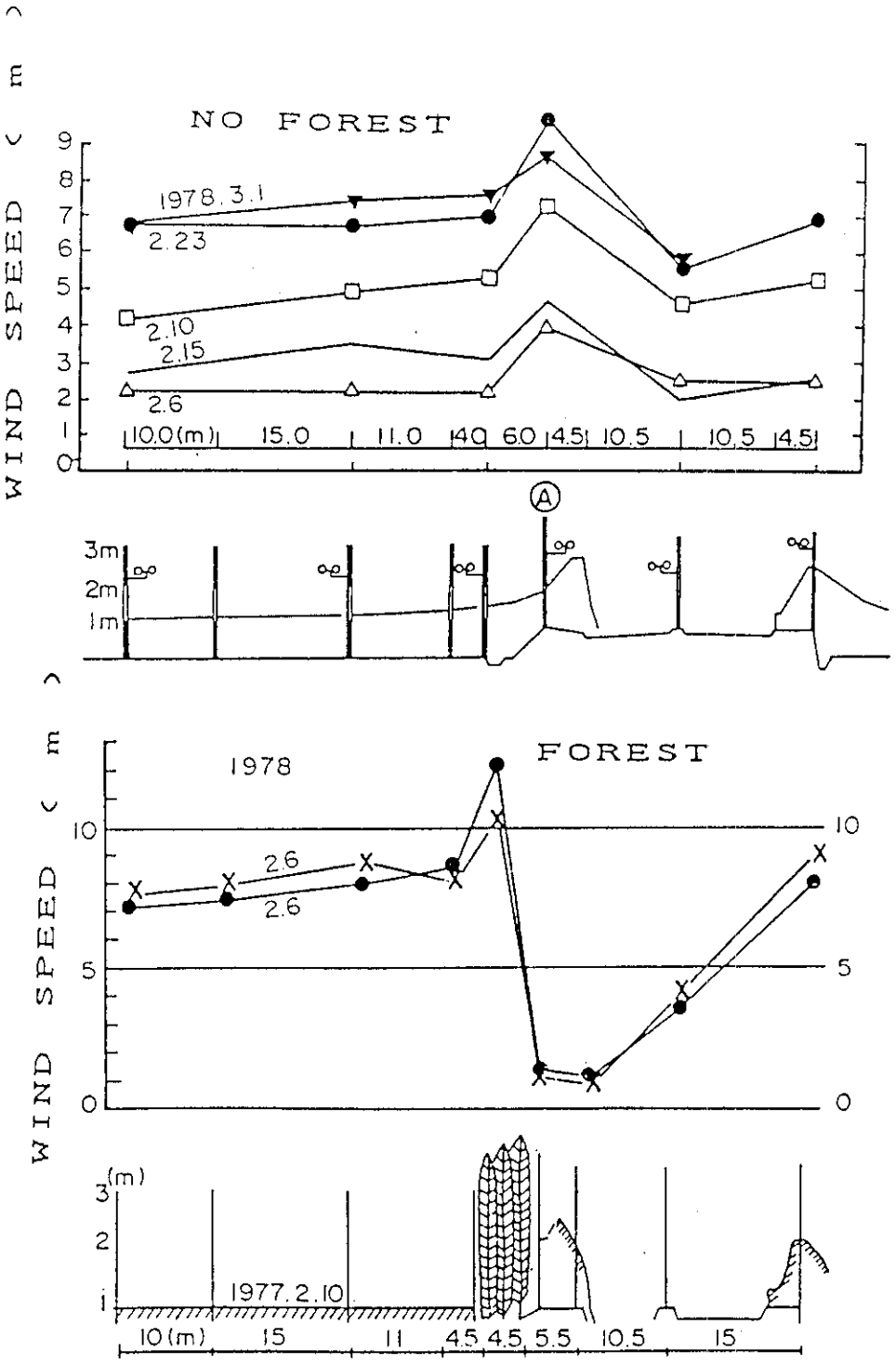

Figure 39 Horizontal wind profiles at 1 m above snow surface in the section of snow break forest and no forest section

図－39 防雪林の有無による風速横断分布（雪面上１m）

Table 2 Mass flux of blowing snow in the section of snow break forest (length of forest: 100 m) and that of no-forest section at two levels above the median of the highway (at Iwamizawa on NHR、１２)

(length of forest:100m)

PRECIPITAION	DATE	TIME	WIND DIRECITION	WIND SPEED (m/s)	SECTION	H=1.3m	H=2.3m	FOREST/NO FOREST
						$(Kgm^{-2}S^{-1})*10^{-4}$		H=1.3m, H=2.3m
little	79. 3. 1	15:06	N	12	FOREST	18.2	26.3	68%, 53%
					NO FOREST	26.9	49.5	
no	〃	15:25	N	13	FOREST	6.12	5.27	58%, 67%
					NO FOREST	10.5	7.82	
light	79. 3. 4	15:28	N	5	FOREST	4.42	7.82	48%, 63%
					NO FOREST	9.18	12.4	

Table 3 Mass flux of blowing snow in the section of snow break forest (length of forest: 520 m) and that of no-forest section at two levels above the median of the highway (at Iwamizawa on NHR、１２)

(length of forest:520m)

PRECIPITAION	DATE	TIME	WIND DIRECITION	WIND SPEED (m/s)	SECTION	H=1.3m	H=2.3m	FOREST/NO FOREST
						$(Kgm^{-2}S^{-1})*10^{-4}$		H=1.3m, H=2.3m
heavy	80. 3. 1	18:12	WNW	9～13	FOREST	6.46	9.01	12%, 16%
					NO FOREST	55.3	55.8	
〃	〃	18:15	WNW	9～13	FOREST	10.4	11.4	24%, 27%
					NO FOREST	43.2	42.8	
〃	〃	18:43	WNW	12～19	FOREST	12.8	17.5	13%, 18%
					NO FOREST	98.3	97.4	

表２、３　吹雪の程度による防雪林の有無による飛雪流量の違い。飛雪流量の多い吹雪ほど防雪林設置効果が大きい。

Table 4 Visibility and visibility fluctuation in the section of snow break forest and in no-forest section at 1.5 m high on the median of the highway at Iwamizawa on NHR １２,

	(Ⅰ)FOREST		(Ⅱ)NO FOREST		(Ⅰ)／(Ⅱ)	
	$\overline{V}$ (m)		$\overline{V}$ (m)		V (m)	
①	1200	31	1090	36	1.10	0.86
②	1130	34	860	42	1.31	0.81
③	1150	32	800	43	1.31	0.74
④	480	51	290	70	1.66	0.73

表－４　防雪林の有無による平均視程と視程変動強度。視程距離が短いほど防雪林による視程障害緩和効果が大きい。

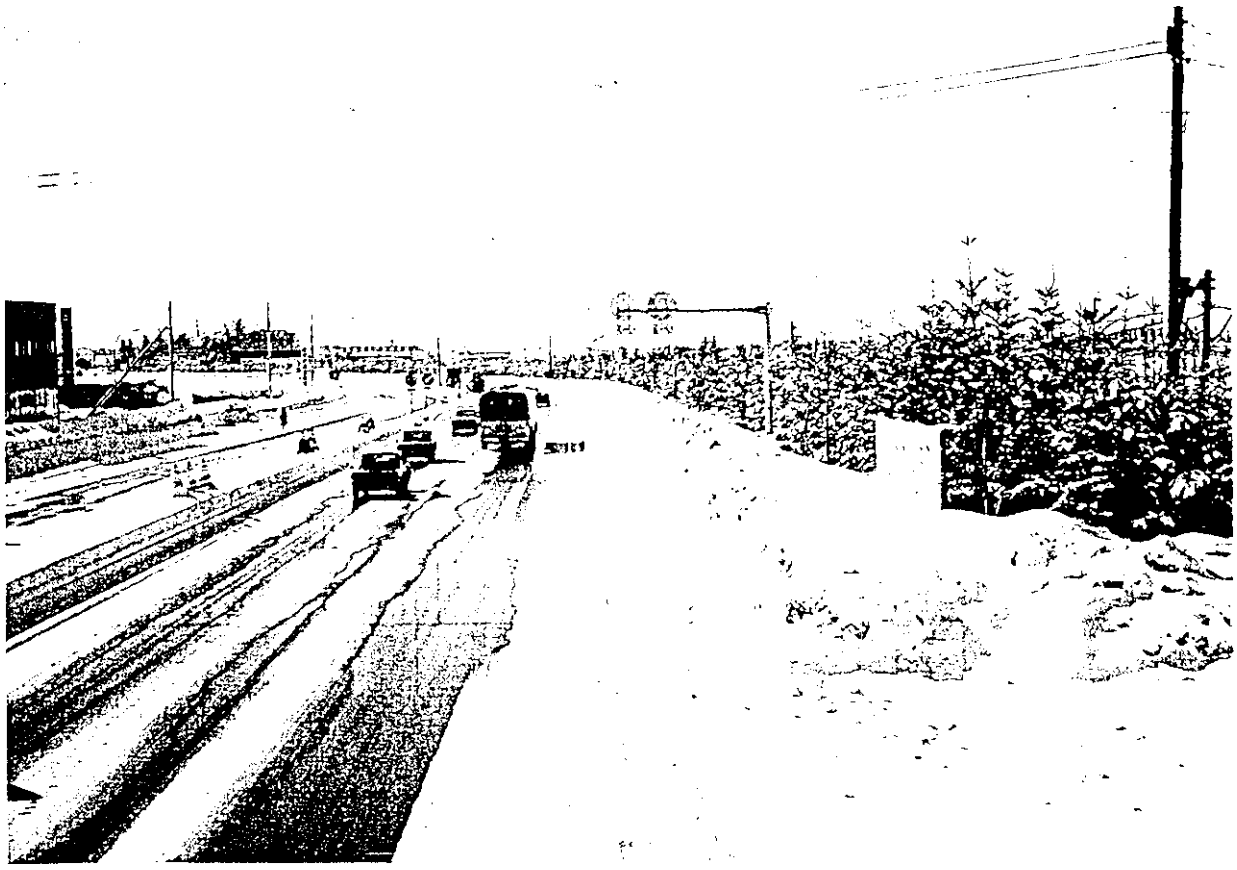

Figure 40 Snow break forest at Iwamizawa on NHR 12

図－40 一般国道 12 号の防雪林設置区間

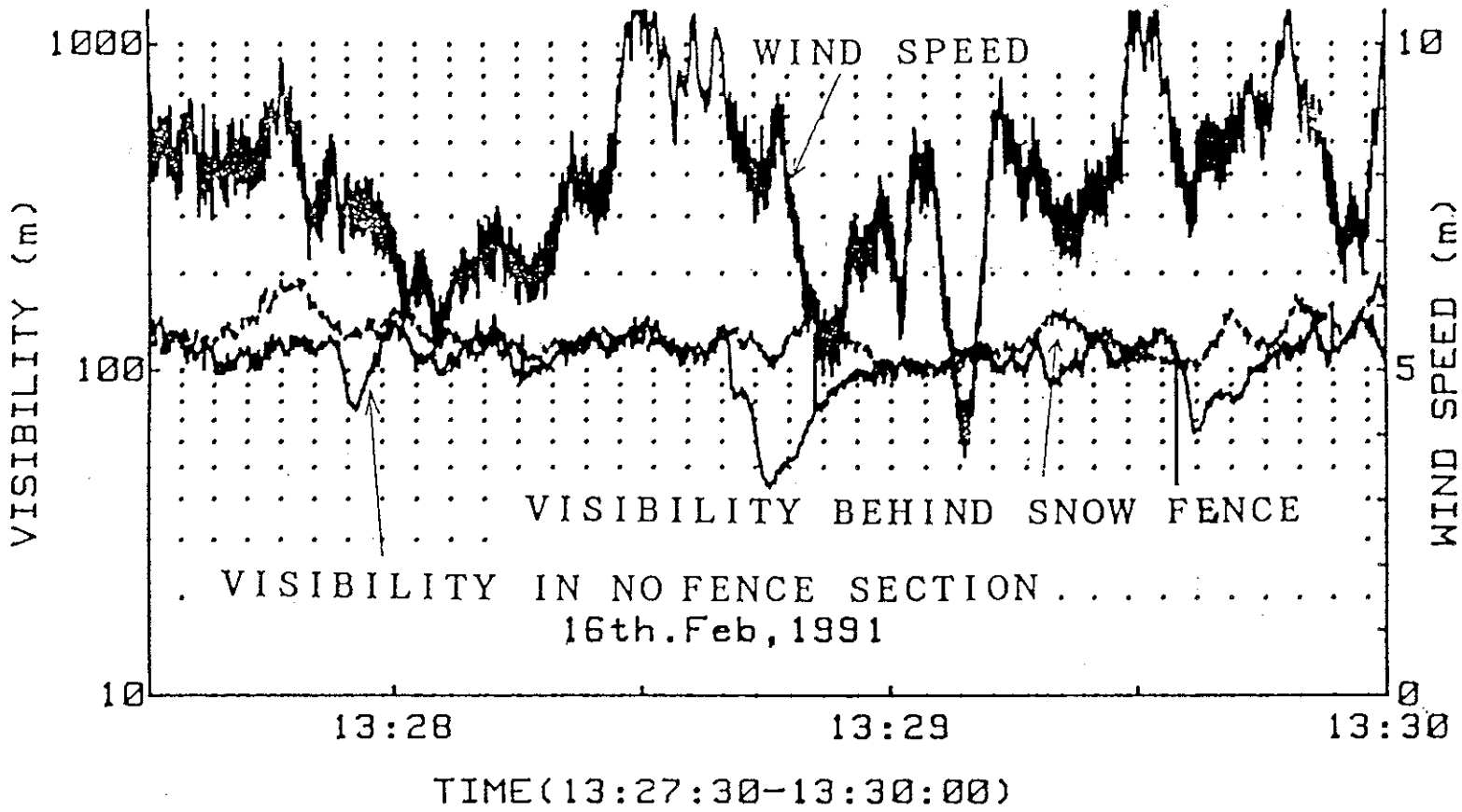

Figure 41 Visibility in blowing snow in snow fence section and in no-fence section

図－41　防雪柵の有無による視程の時間変動

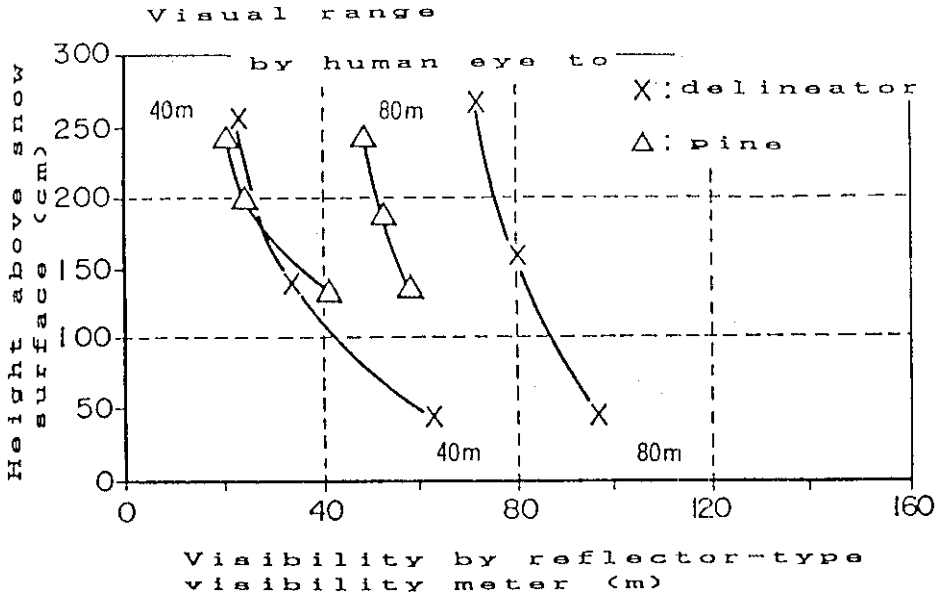

Figure 42 Distance at which delineators and pine trees were recognized at each location on different levels

図－42 視程が変化する時のデリネータと松の木が見える位置と高さ